# AtAIRP2 E3 Ligase Affects ABA and High-Salinity Responses by Stimulating Its ATP1/SDIRIP1 Substrate Turnover[1]

**Tae Rin Oh,[2] Jong Hum Kim,[2] Seok Keun Cho, Moon Young Ryu, Seong Wook Yang, and Woo Taek Kim[3]**

Department of Systems Biology, College of Life Science and Biotechnology, Yonsei University, Seoul 120-749, Korea

**ORCID ID: 0000-0001-5027-4622 (W.T.K.).**



AtAIRP2 is a cytosolic RING-type E3 ubiquitin ligase that positively regulates an abscisic acid (ABA) response in Arabidopsis (*Arabidopsis thaliana*). Yeast two-hybrid screening using AtAIRP2 as bait identified ATP1 (AtAIRP2 Target Protein1) as a substrate of AtAIRP2. ATP1 was found to be identical to SDIRIP1, which was reported recently to be a negative factor in ABA signaling and a target protein of the RING E3 ligase SDIR1. Accordingly, ATP1 was renamed ATP1/SDIRIP1. A specific interaction between AtAIRP2 and ATP1/SDIRIP1 and ubiquitination of ATP1/SDIRIP1 by AtAIRP2 were demonstrated in vitro and in planta. The turnover of ATP1/SDIRIP1 was regulated by AtAIRP2 in cell-free degradation and protoplast cotransfection assays. The ABA-mediated germination assay of *35S:ATP1/SDIRIP1-RNAi/atairp2* double mutant progeny revealed that ATP1/SDIRIP1 acts downstream of AtAIRP2. AtAIRP2 and SDIR1 reciprocally complemented the ABA- and salt-insensitive germination phenotypes of *sdir1* and *atairp2* mutants, respectively, indicating their combinatory roles in seed germination. Subcellular localization and bimolecular fluorescence complementation experiments in the presence of MG132, a 26S proteasome inhibitor, showed that AtAIRP2 and ATP1/SDIRIP1 were colocalized to the cytosolic spherical body, which lies in close proximity to the nucleus, in tobacco (*Nicotiana benthamiana*) leaf cells. The 26S proteasome subunits RPN12a and RPT1 and the molecular chaperones HSP70 and HSP101 were colocalized to these discrete punctae-like structures. These results raised the possibility that AtAIRP2 and ATP1/SDIRIP1 interact in the cytosolic spherical compartment. Collectively, our data suggest that the down-regulation of ATP1/SDIRIP1 by AtAIRP2 and SDIR1 RING E3 ubiquitin ligases is critical for ABA and high-salinity responses during germination in Arabidopsis.

Being sessile, higher plants are exposed to various environmental stresses, such as drought, cold, and high salinity, during their lifetimes. These injurious environmental conditions are major factors that inhibit plant growth and productivity. Plants, however, have developed an exquisite mechanism to mitigate the detrimental effects of such growth conditions (Mehrotra et al., 2014; Verma et al., 2016). Abscisic acid (ABA) is a plant stress hormone that plays a key role in response to abiotic stresses (Zhu, 2002; Yamaguchi-Shinozaki and Shinozaki, 2006; Tuteja, 2007). ABA also regulates various cellular processes during plant development, including seed maturation and germination, transition from the seed to seedling stage, and fruit ripening (Finkelstein et al., 2002; Gomez-Cadenas et al., 2015). The perception and signal transduction of ABA, which involve PYR/PYL/RCAR receptors and a downstream protein phosphatase/kinase enzyme pair, PP2Cs and SnRK2s, have been documented in Arabidopsis (*Arabidopsis thaliana*; Park et al., 2009; Cutler et al., 2010; Rodrigues et al., 2013; Kim, 2014).

The ubiquitin-26S proteasome system (UPS) is a selective proteolytic pathway that eliminates specific target proteins in eukaryotic cells (Dreher and Callis, 2007; Vierstra, 2009; Lyzenga and Stone, 2012; Sadanandom et al., 2012; Stone, 2014; Zhang et al., 2015; Yu et al., 2016). More than 6% of the Arabidopsis proteome has been identified to be involved in the UPS (Vierstra, 2012). Ubiquitin (Ub) is labeled to target proteins by serial reactions of three enzymes, E1 Ub-activating enzyme, E2 Ub-conjugating enzyme, and E3 Ub ligase, in an ATP-dependent manner (Guerra and Callis, 2012; Vierstra, 2012; Kleiger and Mayor, 2014). The largest portion of the UPS comprises E3 ligases, and more than 1,400 different E3 ligases have been predicted in the Arabidopsis genome. This large number of E3 Ub ligases is reasonable, as, in general, they specifically determine the target protein and the

[1] This work was supported by a grant from the National Research Foundation of Korea (project nos. 2014R1A2A2A01003891 and 2017R1A2B2006750) to W.T.K.

[2] These authors contributed equally to the article.

[3] Address correspondence to wtkim@yonsei.ac.kr.

The author responsible for distribution of materials integral to the findings presented in this article in accordance with the policy described in the Instructions for Authors (www.plantphysiol.org) is: Woo Taek Kim (wtkim@yonsei.ac.kr).

T.R.O., J.H.K., S.K.C., and M.Y.R. performed the experiments; T.R.O., J.H.K., S.W.Y, and W.T.K. analyzed the data; T.R.O., J.H.K., and W.T.K. planned the project and wrote the article; W.T.K. supervised the project and complemented the writing.

www.plantphysiol.org/cgi/doi/10.1104/pp.17.00467

  

attachment of a polyubiquitin chain (Kraft et al., 2005; Stone et al., 2005; Vierstra, 2009; Lee and Kim, 2011).

Arabidopsis contains at least 477 Really Interesting New Gene (RING)-type E3 Ub ligases (Kraft et al., 2005; Stone et al., 2005; Vierstra, 2009). Various lines of evidence have amply implicated the participation of RING E3 Ub ligases in ABA-mediated drought stress responses (Lyzenga and Stone, 2012; Stone, 2014; Zhang et al., 2014; Yu et al., 2016). For example, AtAIRP1 and AtAIRP2 positively regulate ABA-dependent stomatal closure and drought tolerance responses (Ryu et al., 2010; Cho et al., 2011). AtAIRP3/LOG2 plays dual functions in an amino acid export pathway and in ABA-mediated drought stress responses (Pratelli et al., 2012; Kim and Kim, 2013a). A drought-induced Cys protease, Responsive to Dehydration21, was identified as a target of AtAIRP3/LOG2 for degradation via the 26S proteasome (Kim and Kim, 2013a). AtAIRP4 was reported to act as a positive regulator of ABA-mediated drought avoidance and, in contrast, as a negative regulator of salt tolerance (Yang et al., 2016). In addition, Arabidopsis RHA2a/RHA2b, AtRDUF1/AtRDUF2, RGLG2, and AtATL78 are positive regulators in the response to dehydration stress (Bu et al., 2009; Li et al., 2011; Cheng et al., 2012; Kim et al., 2012; Kim and Kim, 2013b). However, the detailed underlying mechanisms by which these RING E3 Ub ligases modulate drought tolerance responses remain to be determined. In contrast, DRIP-RING E3 negatively regulates the drought stress response by ubiquitinating and inducing proteasomal degradation of the drought-induced transcription factor DREB2A (Qin et al., 2008). Thus, different RING E3 Ub ligases are critically involved in drought tolerance responses as either positive or negative regulators. These results indicate a potential correlation between the diversity of RING E3s and the sessile lifestyle of higher plants.

SDIR1 (Salt- and Drought-Induced Ring Finger1) was identified as an intramembrane-localized RING E3 Ub ligase in Arabidopsis (Zhang et al., 2007). SDIR1 is a positive factor in stress-responsive ABA signaling. Subsequent study has revealed that SDIR1 is localized to the endoplasmic reticulum (ER) membrane and ubiquitinates SDIRIP1 (SDIR1 Interacting Protein1; Zhang et al., 2015). SDIRIP1 acts upstream of an ABA-responsive transcription factor, ABSCISIC ACID-INSENSITIVE5 (ABI5), but not ABF3 and ABF4, to modulate ABA-mediated seed germination and the high-salinity response. Thus, the RING E3 Ub ligase SDIR1 regulates ABA signaling via the UPS-dependent degradation of SDIRIP1 (Zhang et al., 2015).

AtAIRP2 is a cytosolic RING E3 Ub ligase that positively regulates ABA responses, such as seed germination, stomatal closure, and drought tolerance, in Arabidopsis (Cho et al., 2011). To investigate the mode of action of AtAIRP2 as a positive factor of ABA responses, in this study, we performed yeast two-hybrid screening using AtAIRP2 as bait. Several potential interacting partners of AtAIRP2 were isolated and named ATPs (AtAIRP2 Target Proteins). The Arabidopsis Information Resource database (http://www.arabidopsis.org) analysis showed that ATP1 was identical to SDIRIP1; thus, it was renamed ATP1/SDIRIP1. Our data indicated that ATP1/SDIRIP1 was ubiquitinated by AtAIRP2 and that the stability of ATP1/SDIRIP1 was regulated, at least in part, in an AtAIRP2-dependent manner in vitro and in planta. Both RNA interference-mediated *ATP1/SDIRIP1* knockdown transgenic plants (*35S:ATP1/SDIRIP1-RNAi*) and *35S:ATP1/SDIRIP1-RNAi/atairp2* double mutant lines exhibited hypersensitivity toward ABA during seed germination. These results indicated that ATP1/SDIRIP1 acts downstream of AtAIRP2. The reciprocal overexpression of *SDIR1* and *AtAIRP2* in *atarip2* and *sdir1* knockout mutants, respectively, effectively complemented the ABA- and high salinity-insensitive mutant phenotypes during seed germination, indicating their combinatory roles. Subcellular localization and bimolecular fluorescence complementation (BiFC) experiments in the presence of MG132, an inhibitor of the 26S proteasome complex, showed that AtAIRP2 and ATP1/SDIRIP1 were colocalized to the cytosolic spherical body, which lies in close proximity to the nucleus, in tobacco (*Nicotiana benthamiana*) leaf epidermal cells. The 26S proteasome subunits RPN12a and RPT1 and the molecular chaperones HSP70 and HSP101 were closely associated with these discrete punctae-like structures. These results raised the possibility that AtAIRP2 and ATP1/SDIRIP1 interact in the cytosolic punctate compartment. Collectively, our data indicate that AtAIRP2 plays a positive role in ABA- and high salinity-regulated seed germination through the UPS-dependent downregulation of ATP1/SDIRIP1 in Arabidopsis.

## RESULTS

### ATP1/SDIRIP1 Was Identified as a Target Protein of AtAIRP2

We previously reported that AtAIRP2, a cytosolic RING E3 Ub ligase, positively regulates ABA responses in Arabidopsis (Cho et al., 2011). The T-DNA-inserted *atairp2* knockout mutant progeny showed insensitive phenotypes in ABA-mediated seed germination and stomatal closure and, in contrast, displayed hypersensitivity in the response to drought stress compared with that in wild-type plants. To elucidate the mechanism underlying the action of AtAIRP2 as a positive factor in ABA responses, in this study, we attempted to isolate putative substrate proteins of AtAIRP2 and conducted yeast two-hybrid screening.

In our yeast two-hybrid screening, the full-length *AtAIRP2* cDNA clone was fused with a pGBKT7 vector and used as bait. A cDNA library was prepared from 3-d-old etiolated seedlings, cloned into pGADT7, and used as prey. The bait and prey plasmids were cotransformed into yeast strain AH109 and cultured in three-minus selection medium (SD/-Trp/-Leu/-His) for 3 d. Several positive yeast colonies were identified. The cDNA clones encoding putative interacting partners of AtAIRP2 were isolated from the corresponding

yeast cells and named ATPs. DNA sequence analysis revealed that, among several potential ATPs, ATP1 (At5g51110; GenBank accession no. NM_124490) was identical to SDIRIP1 (Zhang et al., 2015). SDIRIP1 was initially identified as a chloroplast-localized type 2 pterin-4$\alpha$-carbinolamine dehydratase (PCD) homolog with an unknown function (Naponelli et al., 2008). Recently, Zhang et al. (2015) reported that SDIRIP1 is a target protein of the ER membrane-localized RING E3 Ub ligase SDIR1. SDIR1 acted as a positive factor in stress-responsive ABA signaling and ubiquitinated SDIRIP1, which resulted in the UPS-dependent degradation of SDIRIP1. Therefore, ATP1 was renamed ATP1/SDIRIP1.

To confirm the interaction of AtAIRP2 with ATP1/SDIRIP1, a yeast two-hybrid assay was repeated under more stringent conditions. As shown in Figure 1A, AtAIRP2 and ATP/SDIRIP1 exhibited strong interaction on four-minus selection medium (SD/-Trp/-Leu/-His/-Ade). Interaction between AtAIRP2 and ATP1/SDIRIP1 was further investigated using an in vitro pull-down assay. Bacterially expressed MBP-AtAIRP2 and 6×His-3×HA-ATP1/SDIRIP1 recombinant proteins were coincubated with an amylose affinity matrix. The bound protein was eluted from the amylose resin using 20 mM maltose and subjected to immunoblot analysis with anti-MBP and anti-HA antibodies. Figure 1B shows that 6×His-3×HA-ATP1/SDIRIP1 was pulled down from the amylose affinity resin by MBP-AtAIRP2, indicating the physical interaction of AtAIRP2 with ATP1/SDIRIP1 in vitro. We next performed an in vivo coimmunoprecipitation (co-IP) assay. The *35S:2×Flag-AtAIRP2* and *35S:ATP1/SDIRIP1-3×Myc* constructs were transiently expressed in tobacco leaves via an *Agrobacterium tumefaciens*-meditated transformation method. Leaf crude extracts (1 mg of protein) were prepared and immunoprecipitated with anti-Flag affinity gel matrix. ATP1/SDIRIP1-3×Myc was precipitated by anti-Flag antibody in an extract of leaves expressing 2×Flag-AtAIRP2 (Fig. 1C), indicating that AtAIRP2 interacts with ATP1/SDIRIP1 in planta.

To further examine whether ATP1/SDIRIP1 is a target protein of AtAIRP2, we carried out a ubiquitination assay. Recombinant 6×His-ATP1/SDIRIP1-3×Myc protein was incubated with MBP-AtAIRP2 at 30°C for 1 h in the presence or absence of Ub, ATP, E1 (UBA1), and E2 (UBC8). The reaction mixtures were subjected to immunoblotting using anti-Myc antibody. The results presented in Figure 1D show that coincubation of

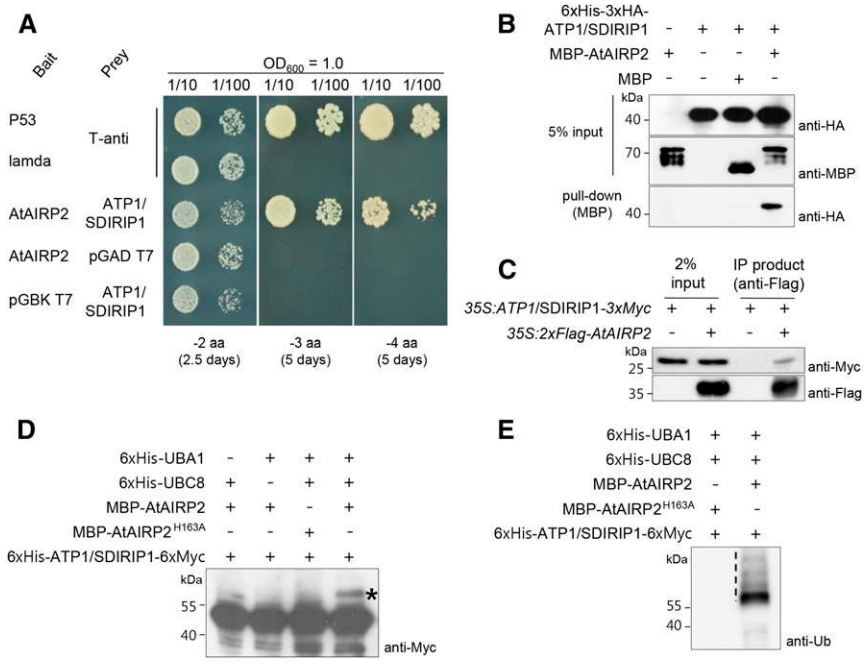


**Figure 1.** AtAIRP2 interacts with ATP1/SDIRIP1. A, Yeast two-hybrid assay. *AtAIRP2* and *ATP1/SDIRIP1* were cloned into pGBKT7 and pGADT7, respectively. Yeast AH109 cells were cotransformed with a combination of the indicated plasmids. The yeast cells were plated onto SD/-Trp/-Leu/-His/-Ade medium and allowed to grow for 4 d at 30°C. p53 + T-antigen was used as a positive control, and lambda + T-antigen was used as a negative control. aa, Amino acids. B, In vitro pull-down assay. Bacterially expressed 6×His-3×HA-ATP1 and MBP-AtAIRP2 fusion proteins were coincubated in the presence of an amylose gel matrix. The resin-bound proteins were eluted with 2× SDS sample buffer and subjected to immunoblot analysis using anti-HA and anti-MBP antibodies. C, In vivo co-IP assay. The *35S:ATP1/SDIRIP1-3×Myc* and *35S:2×Flag-AtAIRP2* constructs were infiltrated into tobacco leaves. Leaf crude extract (1 mg of protein) was immunoprecipitated with anti-Flag affinity gel matrix. The bound proteins were eluted, separated by SDS-PAGE, and detected with anti-Flag or anti-Myc antibody. D and E, In vitro target ubiquitination assays. Recombinant 6×His-ATP1/SDIRIP1-6×Myc protein was incubated in the presence or absence of E1, E2, MBP-AtAIRP2, or MBP-AtAIRP2$^{H163A}$ for 1 h and subjected to immunoblotting using anti-Myc (D) and anti-Ub (E) antibodies. The asterisk indicates the shifted high-molecular-mass band. The vertical dashed line indicates a ubiquitinated smear ladder.

6×His-ATP1/SDIRIP1-6×Myc and MBP-AtAIRP2 produced a high-molecular-mass shifted band. Exclusion of either E1 or E2 from the reaction mixtures abolished the shifted band. Immunoblot analysis using anti-Ub antibody yielded ubiquitinated smear bands (Fig. 1E). An MBP-AtAIRP2$^{H163A}$ single amino acid substitution mutant protein, in which a conserved His residue in the RING motif was changed to an Ala residue, failed to ubiquitinate 6×His-ATP1/SDIRIP1-6×Myc (Fig. 1, D and E). Taken together, these results indicate that ATP1/SDIRIP1 is a target protein of cytosolic AtAIRP2 (Fig. 1) in addition to the ER-localized AtSDIR1 RING E3 Ub ligase (Zhang et al., 2015).

### The Turnover of ATP1/SDIRIP1 Was Regulated by AtAIRP2

Given that ATP1/SDIRIP1 was ubiquitinated by ABA-induced AtAIRP2 (Fig. 1), we presumed that the turnover of ATP1/SDIRIP1 is regulated by AtAIRP2 in ABA and 26S proteasome-dependent manners. To investigate this possibility, a cell-free degradation assay was performed. The 6×His-ATP1/SDIRIP1-6×Myc protein was incubated with protein crude extracts prepared from wild-type leaves with or without ABA (50 $\mu$M), and its degradation pattern was monitored. As shown in Figure 2A, 6×His-ATP1/SDIRIP1-6×Myc was more rapidly degraded in the ABA-treated leaf extracts compared with the mock-treated extracts, suggesting that the turnover of 6×His-ATP1/SDIRIP1-6×Myc is ABA dependent.

Next, the 6×His-ATP1/SDIRIP1-6×Myc protein was incubated with protein crude extracts prepared from wild-type leaves in the absence or presence of MG132 (40 $\mu$M), an inhibitor of the 26S proteasome. The results showed that the level of 6×His-ATP1/SDIRIP1-6×Myc decreased over time (0–2 h) in the wild-type cell-free extracts. After 1 h of incubation, approximately 74% of the protein was degraded (left, Fig. 2B). After 2 h, only approximately 13% of the protein was detected. The degradation pattern of 6×His-ATP1/SDIRIP1-6×Myc was akin to that of RGA1-2×Flag, which was regulated by the UPS (Dill et al., 2004; Lee et al., 2010). In contrast, the degradation of both 6×His-ATP1/SDIRIP1-6×Myc and RGA1-2×Flag was almost completely suppressed in the presence of MG132. These results, along with those presented by Zhang et al. (2015), indicate that the stability of ATP1/SDIRIP1 is subject to regulation by the UPS.

The results also show that ATP1/SDIRIP1 was more stable with cell-free extracts of the *atairp2-1* knockout mutant compared with the wild-type extracts. After a 1-h incubation, more than ~63% of 6×His-ATP1/SDIRIP1-6×Myc was detectable in the mutant crude extracts (middle, Fig. 2B). After 2 h of incubation, we could still detect approximately 19% of the protein. Thus, the degradation of ATP1/SDIRIP1 was retarded with *atairp2* cell-free extracts. In contrast, the 6×His-ATP1/SDIRIP1-6×Myc level was more rapidly reduced with the crude extracts of the *35S:AtAIRP2-sGFP*-overexpressing line relative to the wild type: only approximately 11% and less than 1% of the protein were detected after 1- and 2-h incubations, respectively (right, Fig. 2B). Under our experimental conditions, the apparent half-lives of 6×His-ATP1/SDIRIP1-6×Myc were 33.4, 66.8, and 19.8 min in wild-type, *atairp2-1*, and *35S:AtAIRP2-sGFP* cell-free extracts, respectively (Fig. 2C). This indicates that ATP1/SDIRIP1 was more stable with *atairp2* knockout mutant cell-free extracts and, in contrast, less stable with *AtAIRP2*-overexpressing extracts than with the wild type. Decreases in the ATP1/SDIRIP1 level were effectively inhibited by MG132 in cell-free extracts of both the *atairp2* mutant and *AtAIRP2* overexpressors (Fig. 2B). In addition, the proteasome-dependent degradation profiles of the RGA1-2×Flag protein in the wild-type cell-free extracts were indistinguishable from those in the *atairp2* mutant and *35S:AtAIRP2-sGFP* transgenic cell-free extracts, indicating that the UPS-mediated degradation of RGA-1 was independent of AtAIRP2. These results indicate that the UPS-dependent degradation of ATP1/SDIRIP1 was regulated, at least in part, by AtAIRP2 RING E3 Ub ligase.

The AtAIRP2-dependent turnover of ATP1/SDIRIP1 was further investigated using a protoplast transient expression system. The *35S:ATP1/SDIRIP1-3×Myc* construct was transfected into the wild-type protoplasts along with *35S:AtAIRP2-sGFP* or *35S:sGFP*. *35S:DSred2* was used as a cotransfection control for equal loading. After overnight incubation, the protoplasts were harvested and the total crude extracts were subjected to immunoblot analysis with anti-Myc and anti-GFP antibodies. The results revealed that, in the presence of AtAIRP2-sGFP, the ATP1/SDIRIP1 level decreased markedly by up to approximately 30% compared with the control (Fig. 2D). The reduction of ATP1/SDIRIP1 was again hampered by MG132 (Fig. 2E). This indicates that the degradation of ATP1/SDIRIP1 was promoted by AtAIRP2 in a UPS-dependent manner in the protoplasts. The amount of DSred2 was constant regardless of the presence of AtAIRP2. Overall, the results of protein degradation assays provided evidence that the turnover of ATP1/SDIRIP1 is regulated by AtAIRP2 in a UPS-dependent manner.

### ATP1/SDIRIP1 Works Downstream of AtAIRP2

To examine whether ATP1/SDIRIP1 works downstream of AtAIRP2, RNA interference-mediated *ATP1/SDIRIP1* knockdown transgenic plants (*35S:ATP1/SDIRIP1-RNAi*) were constructed (Supplemental Fig. S1) and the ABA-related phenotypes were compared with those of wild-type and *atairp2* knockout mutant plants. As found previously (Cho et al., 2011), the *atairp2-1* line displayed an insensitive phenotype toward ABA (0.5–1 $\mu$M) in terms of seed germination (Fig. 3A). In contrast, the *35S:ATP1/SDIRIP1-RNAi* plants (independent lines 1 and 2) were hypersensitive to ABA (Fig. 3A). Under our experimental conditions, the

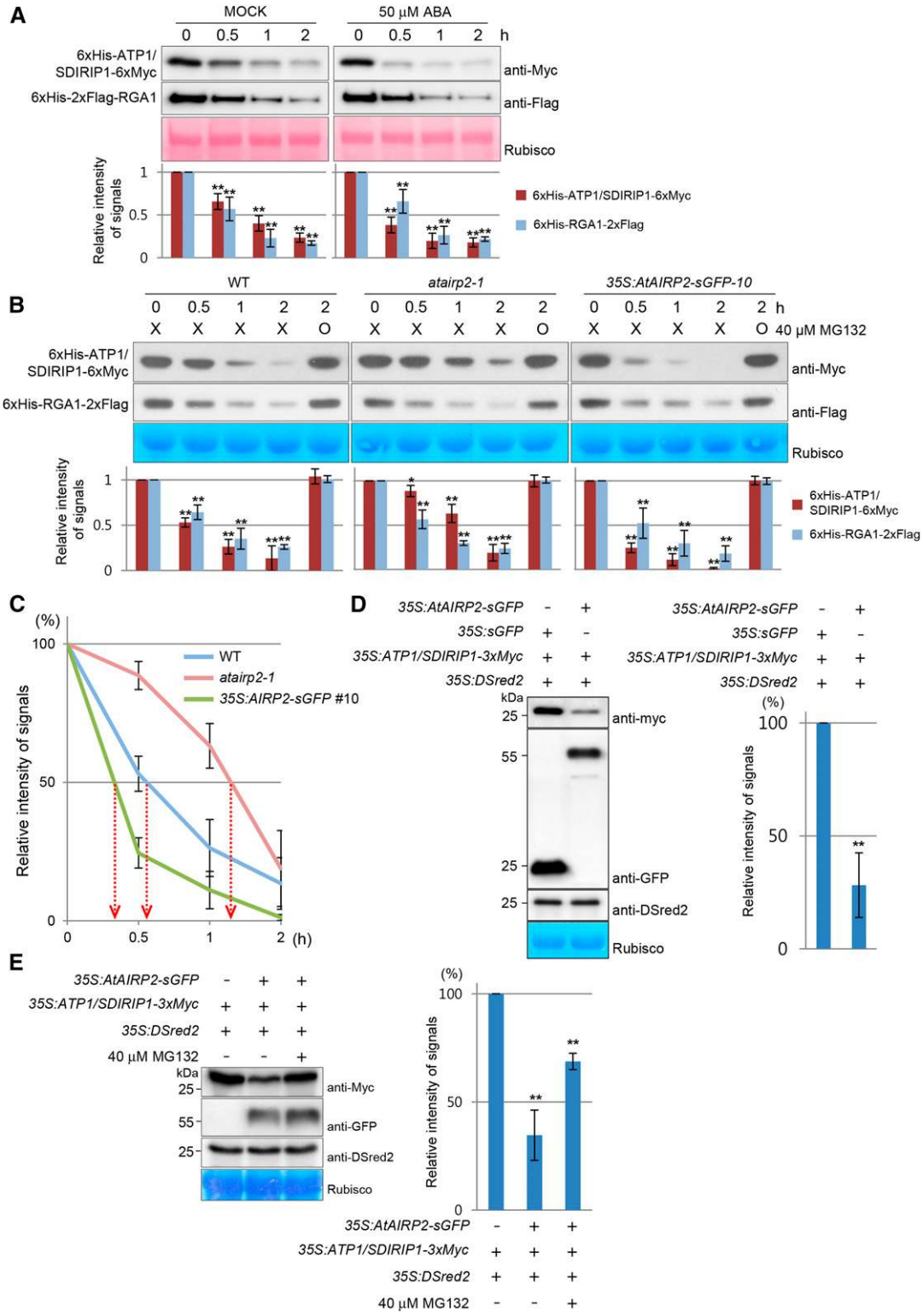


**Figure 2.** The turnover of ATP1/SDIRIP1 was regulated by AtAIRP2 in a 26S proteasome-dependent manner. A and B, In vitro cell-free degradation assay of ATP1/SDIRIP1. Bacterially expressed 6×His-ATP1/SDIRIP1-6×Myc and 6×His-RGA1-2×Flag were incubated with leaf crude extracts prepared from 14-d-old wild-type plants treated with mock or 50 $\mu$M ABA (6 h) for the indicated time periods (A). The recombinant ATP1/SDIRIP1 and RGA1 were incubated with leaf crude extracts prepared from 14-d-old wild-type (WT), *35S:AtAIRP2-sGFP*-overexpressing, or *atairp2-1* mutant plants in the absence (0, 0.5, 1, and 2 h) or presence (2 h) of 40 $\mu$M MG132 (B). The protein levels were measured by immunoblot analysis using anti-Myc and anti-Flag antibodies. DSred2

radicle emergence rates of the wild-type, *atairp2-1*, and *35S:ATP1/SDIRIP1-RNAi* plants were 52% ± 4%, 72% ± 10.5%, and 25.3% ± 4.6% (line 1) − 30.6% ± 6.1% (line 2), respectively, in response to 0.5 μM ABA (Fig. 3B). In the presence of 1 μM ABA, 15% ± 5.6% and 30% ± 8.7% of the wild-type and *atairp2-1* mutant seeds were still able to germinate, whereas only 4.6% ± 3% (line 1) and 5.9% ± 2% (line 2) of the *35S:ATP1/SDIRIP1-RNAi* seeds could germinate. We obtained similar results with respect to the rates of cotyledon greening: *atairp2-1* showed insensitivity and *35S:ATP1/SDIRIP1-RNAi* progeny were hypersensitive to ABA (Fig. 3C), which is consistent with the notion that ATP1/SDIRIP1 acts as a negative factor in response to ABA.

To examine the epistasis between AtAIRP2 and ATP1/SDIRIP1, *35S:ATP1/SDIRIP1-RNAi/atairp2* double mutant lines were generated by crossing *35S:ATP1/SDIRIP1-RNAi* and *atairp2* plants (Supplemental Fig. S2). In response to ABA (0.5–1 μM) treatments, the germination rates of the *35S:ATP1/SDIRIP1-RNAi/atairp2* double mutant exhibited hypersensitive phenotypes, which were more reminiscent of those of *35S:ATP1/SDIRIP1-RNAi* knockdown plants than those of *atairp2* (Fig. 3). These results indicate that AtARIP2 is epistatic to ATP1/SDIRIP1 in ABA-dependent seed germination. Based on these observations, we conclude that ATP1/SDIRIP1 is a target protein of the RING E3 Ub ligase AtAIRP2 and exerts its negative effects on the ABA signaling pathway downstream of AtAIRP2.

### Functional Relationship between AtAIRP2 and SDIR1 RING E3 Ub Ligases

Both AtAIRP2 and SDIR1 play positive roles in ABA-dependent processes, including seed germination and drought and high-salt stress responses (Zhang et al., 2007; Cho et al., 2011). Our data indicate that ATP1/SDIRIP1 is a target protein of AtAIRP2 (Figs. 1–3) in addition to SDIR1 (Zhang et al., 2015). With these results in mind, we conjectured that AtAIRP2 and SDIR1 play a combinatory role in ABA signaling by ubiquitinating a common substrate protein, ATP1/SDIRIP1.

To examine this hypothesis, the AtAIRP2-dependent turnover of ATP1/SDIRIP1 was monitored in the presence or absence of SDIR1 via a protoplast transient expression system. The *35S:ATP1/SDIRIP1-3×Myc* construct was transfected into wild-type or *atairp2-1* protoplasts along with *35S:DSred2*. DSred2 was used as an equal loading control. As indicated in Figure 4, A and B, the ATP1/SDIRIP1-3×Myc level was approximately 1.4-fold higher in the *atairp2-1* protoplasts relative to the wild-type protoplasts. When *35S:ATP1/SDIRIP1-3×Myc* was introduced into the *atairp2-1* protoplasts together with *35S:AtAIRP2-sGFP*, the amount of ATP1/SDIRIP1-3×Myc was reduced to ~60% compared with the control (Fig. 4, A and B). In addition, when the *35S:ATP1/SDIRIP1-3×Myc* and *35S:2×Flag-SDIR1* constructs were cotransfected into the *atairp2-1* protoplasts, only approximately 40% of ATP1/SDIRIP1-3×Myc was detected. These results indicate that SDIR1 effectively supplemented AtAIRP2 in terms of ATP1/SDIRIP1 degradation.

An identical experiment was carried out with *sdir1-1* mutant protoplasts. As expected, the ATP1/SDIRIP1-3×Myc level increased by approximately 1.8-fold in the *sdir1-1* protoplasts compared with the wild type (Fig. 4, C and D). The level of ATP1/SDIRIP1-3×Myc was reduced to ~50% and 65% that of the control when *35S:ATP1/SDIRIP1-3×Myc* was cointroduced into *sdir1-1* protoplasts along with *35S:2xFlag-SDIR1* and *35S:AtAIRP2-sGFP*, respectively (Fig. 4, C and D). Thus, it appeared that AtAIRP2 supplemented SDIR1 in the degradation of ATP1/SDIRIP1.

We next conducted reciprocal complementation tests. The *SDIR1* and *AtAIRP2* genes were ectopically expressed in *atairp2-1* and *sdir1-1* mutant lines, respectively. Independent complementation transgenic plants (*atairp2-1/35S:2×Flag-SDIR1* and *sdir1-1/35S:AtAIRP2-sGFP*) were selected. The expression of *SDIR1* and *AtAIRP2* transgenes was detected in *atairp2-1/35S:2×Flag-SDIR1* (lines 1 and 5) and *sdir1-1/35S:AtAIRP2-sGFP* (lines 4 and 11) T3 complementation lines, respectively, by RT-PCR (Fig. 5A) and immunoblotting (Fig. 5B). These complementation progeny were used in the phenotypic analysis of ABA responses to examine if mutant phenotypes were reciprocally rescued. As described previously (Zhang et al., 2007; Cho et al., 2011), both *atairp2-1* and *sdir1-1* mutants were hyposensitive to ABA (0.5–1 μM) compared with wild-type seedlings during the germination

**Figure 2.** (*Continued.*)
and Rubisco large subunit were used as loading controls. The time-dependent degradation patterns of each protein were quantified using ImageJ software. Results are presented as means ± SD (*, $P < 0.05$ and **, $P < 0.01$, Student's *t* test) of three independent biological replicates. C, Apparent half-lives of 6×His-ATP1/SDIRIP1-6×Myc in the cell-free crude extracts. The graph shows the time-dependent decrease in the relative amount of 6×His-ATP1/SDIRIP1-6×Myc in the cell-free degradation assay. The levels of proteins were quantified by calculation of band intensities using ImageJ software. D and E, Protoplast cotransfection assay. The *35S:AtAIRP2-sGFP*, *35S:sGFP*, *35S:ATP1/SDIRIP1-3×Myc*, and *35S:DSred2* constructs (D) or the *35S:AtAIRP2-sGFP*, *35S:ATP1/SDIRIP1-3×Myc*, and *35S:DSred2* constructs (E) were introduced into Arabidopsis leaf protoplasts by the polyethylene glycol-mediated transformation method. The transformed protoplasts were incubated in washing and incubation solution (4 mM MES, pH 5.7, 0.5 M mannitol, and 20 mM KCl) at 22°C under conditions of continuous light. After 16 h of incubation, protoplasts were incubated with or without 40 μM MG132 for 2 h (E). Total proteins were extracted from the protoplasts and subjected to immunoblotting with anti-Myc, anti-GFP, and anti-DSred2 antibodies. Results are presented as means ± SD (**, $P < 0.01$, Student's *t* test) of three independent biological replicates.

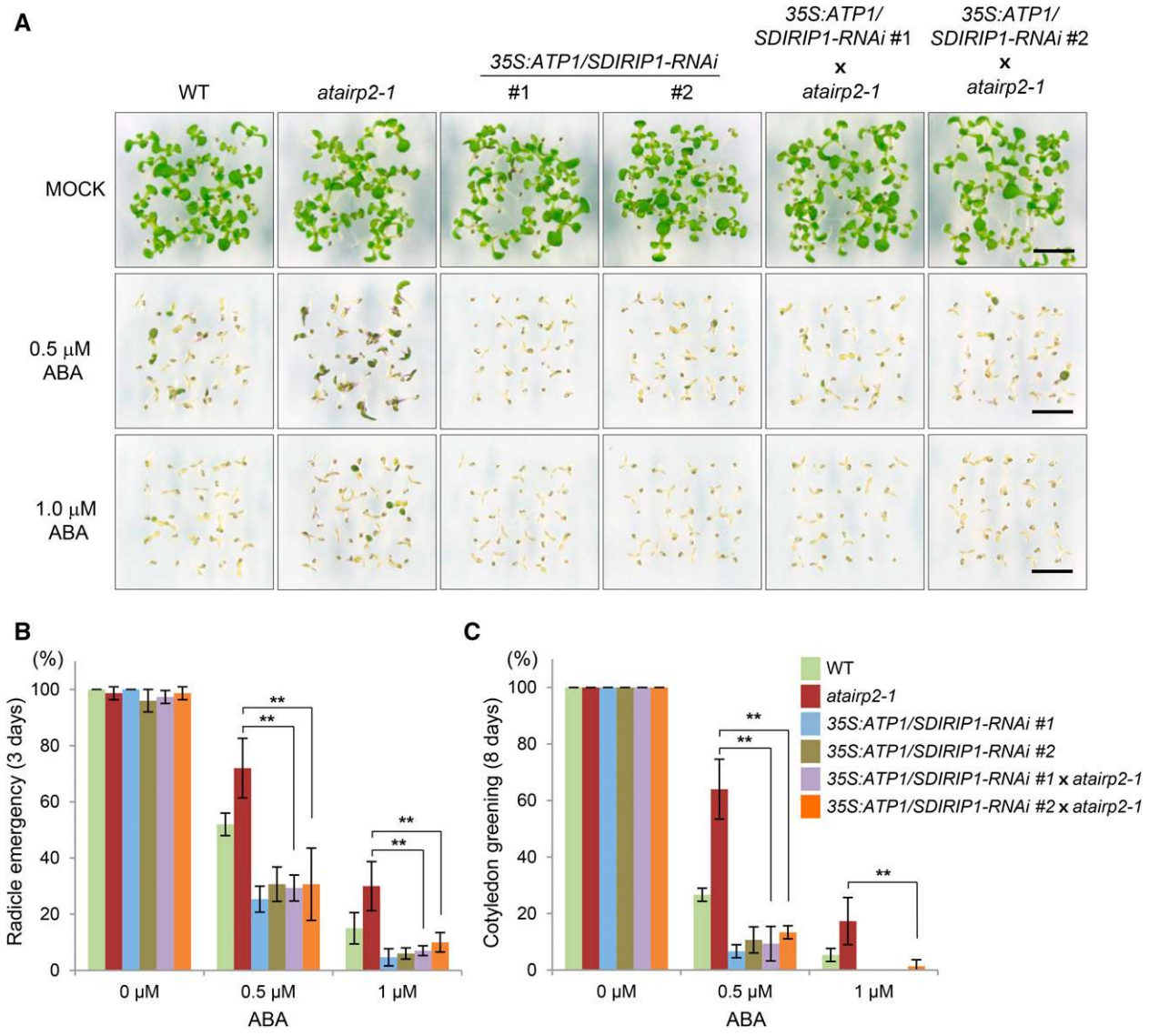


**Figure 3.** AtAIRP2 is epistatic to ATP1/SDIRIP1 in ABA-mediated seed germination. A, Germination assays of wild-type (WT), *atairp2-1*, *35S:ATP1/SDIRIP1-RNAi* (independent lines 1 and 2), and *35S:ATP1/SDIRIP1-RNAi/atairp2-1* plants in response to ABA. Sterilized seeds were imbibed in water for 2 d at 4°C and incubated on Murashige and Skoog (MS) medium in the presence of different concentrations (0, 0.5, and 1 $\mu$M) of ABA at 22°C under a 16-h-light/8-h-dark photoperiod. Bars = 0.5 cm. B and C, Germination percentages were determined in terms of radicle emergence 3 d after germination (B) and cotyledon greening 8 d after germination (C). Results are presented as means ± SD (**, $P < 0.01$, Student's *t* test) of three independent biological replicates ($n = 25$).

stage (Fig. 5C). However, *atairp2-1/35S:2×Flag-SDIR1* and *sdir1-1/35S:AtAIRP2-sGFP* double transgenic lines displayed hypersensitivity to ABA in their seed germination. After incubation with 0.5 $\mu$M ABA, the percentages of radicle emergence for wild-type, *atairp2-1*, *atairp2-1/35S:2xFlag-SDIR1* (lines 1 and 5), *sdir1-1*, and *sdir1-1/35S:AtAIRP2-sGFP* (lines 4 and 11) plants were 44% ± 4%, 70.6% ± 10%, 20% ± 4%, 24% ± 8%, 80% ± 8%, 25.3% ± 6.1%, and 29.3% ± 2.3%, respectively (Fig. 5D). In addition, the percentages of cotyledon greening were 30.6% ± 8.3%, 68% ± 18.3%, 10.7% ± 4.6%, 8% ± 4%, 82.6% ± 14%, 16% ± 4%, and 21.3% ± 9.2%, respectively (Fig. 5E). Thus, the ABA-insensitive phenotypes of *atairp2-1* and *sdir1-1* young seedlings were efficiently rescued by reciprocal overexpression of *SDIR1* and *AtAIRP2*, respectively.

Analysis of salt stress responses also showed that salinity-insensitive phenotypes of single mutant seedlings (*atairp2-1* and *sdir1-1*) were reciprocally rescued in complementation seedlings (*atairp2-1/35S:2×Flag-SDIR1* and *sdir1-1/35S:AtAIRP2-sGFP*). The results presented in Figure 6A show that *atairp2-1* and *sdir1-1* were insensitive to NaCl (100 and 150 mM) during

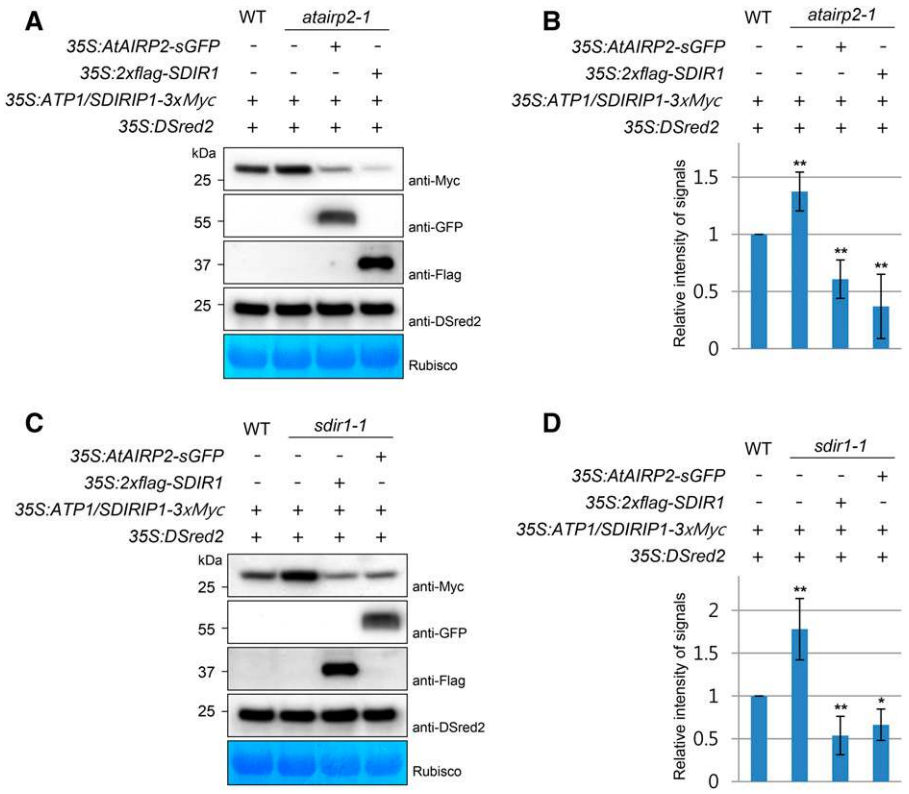


**Figure 4.** Combinatorial down-regulation of ATP1/SDIRIP1 by AtAIRP2 and SDIR1 RING E3 Ub ligases. A and C, The indicated combinations of *35S:ATP1/SDIRIP1-3×Myc*, *35S:AtAIRP2-sGFP*, *35S:2×Flag-SDIR1*, and *35S:DSred2* constructs were transformed into the protoplasts prepared from wild-type (WT; A and C), *atairp2-1* (A), or *sdir1-1* (C) leaves and incubated in washing and incubation solution for 16 h at 22°C under conditions of continuous light. The protein levels were examined by immunoblot analysis with anti-Myc, anti-GFP, anti-Flag, and anti-DSred2 antibodies. B and D, Protein levels were quantified by calculation of band intensities using ImageJ software. DSred2 and Rubisco large subunit were used as loading controls. Bars represent means ± SE (*, $P < 0.05$ and **, $P < 0.01$, Student's *t* test) of three independent biological replicates.

their seed germination relative to the wild type. After 100 mM NaCl treatment, the germination percentages of the wild type, *atairp2-1*, and *sdir1-1* were 54.7% ± 6.1%, 77.3% ± 9.2%, and 88% ± 10.6%, respectively, in radicle emergence (Fig. 6B) and 58.7% ± 10%, 81.3% ± 6.1%, and 92% ± 4%, respectively, in cotyledon greening (Fig. 6C). In contrast, sensitivity toward high salinity was restored in both *atairp2-1/35S:2×Flag-SDIR1* and *sdir1-1/35S:AtAIRP2-sGFP* progeny. With 100 mM NaCl, the germination percentages of *atairp2-1/35S:2×Flag-SDIR1* (lines 1 and 5) and *sdir1-1/35S:AtAIRP2-sGFP* (lines 4 and 11) were reduced to 29.3% ± 8.3% – 32% ± 9.2% and 37.3% ± 10% – 36% ± 8%, respectively, in radicle emergence (Fig. 6B) and to 37.3% ± 2.3% – 40% ± 4% and 46.7% ± 6.1% – 52% ± 10.5%, respectively, in cotyledon greening (Fig. 6C).

Furthermore, qRT-PCR analysis showed that *ABI5* transcript levels are restored by the ectopic expression of *AtAIRP2* and *SDIR1* in *sdir1* and *atairp2* mutants, respectively (Fig. 6D). This further suggests the reciprocal actions of AtAIRP2 and SDIR1 in the expression of *ABI5*. Overall, these results indicate that the cellular roles of AtAIRP2 and SDIR1 were reciprocally supplemented by SDIR1 and AtAIRP2, respectively, in the UPS-dependent ATP1/SDIRIP1 degradation (Fig. 4), during the germination stage in response to ABA (Fig. 5) and high salinity (Fig. 6, A–C), and in *ABI5* expression (Fig. 6D). These results suggest that AtAIRP2 and SDIR1 play a combinatory role in ABA signaling and the response to high salt in Arabidopsis.

### Interaction of AtAIRP2 and ATP1/SDIRIP1 in the Cytosolic Spherical Compartment in Tobacco Leaf Epidermal Cells

The aforementioned results indicate that the mode of the negative action of ATP1/SDIRIP1 on ABA signaling is subject to control by AtAIRP2 in a 26S proteasome-dependent manner. It should be noted that AtAIRP2 was detected in the cytosolic fraction (Cho et al., 2011), whereas ATP1/SDIRIP1 was reported to be present mainly in chloroplasts (Naponelli et al., 2008). Minor localization of ATP1/SDIRIP1 to the nucleus and cell periphery also was reported (Zhang et al., 2015). Thus, we reexamined the subcellular localization of AtAIRP2 and ATP1/SDIRIP1. The *35S:AtAIRP2-sGFP* and *35S:ATP1/SDIRIP1-mRFP* constructs were introduced into tobacco leaves by means of *A. tumefaciens*-mediated transformation, and fluorescence signals in the epidermal cells were analyzed using a confocal microscope. Consistent with previous results, the localization signals for AtAIRP2-sGFP and ATP1/SDIRIP1-mRFP were detected predominantly in the cytosol and chloroplasts, respectively, in tobacco leaf cells (left in Fig. 7A). Given that the cellular level of ATP1/SDIRIP1 is regulated by the UPS (Figs. 2 and 4), we hypothesized that the localization pattern of ATP1/SDIRIP1 might be altered after the inhibition of 26S proteasome activity. To examine this possibility, a subcellular localization assay was repeated in the presence of MG132 (20 μM for 4 h). Intriguingly, additional localization signals for AtAIRP2-sGFP and ATP1/SDIRIP1-mRFP were detected

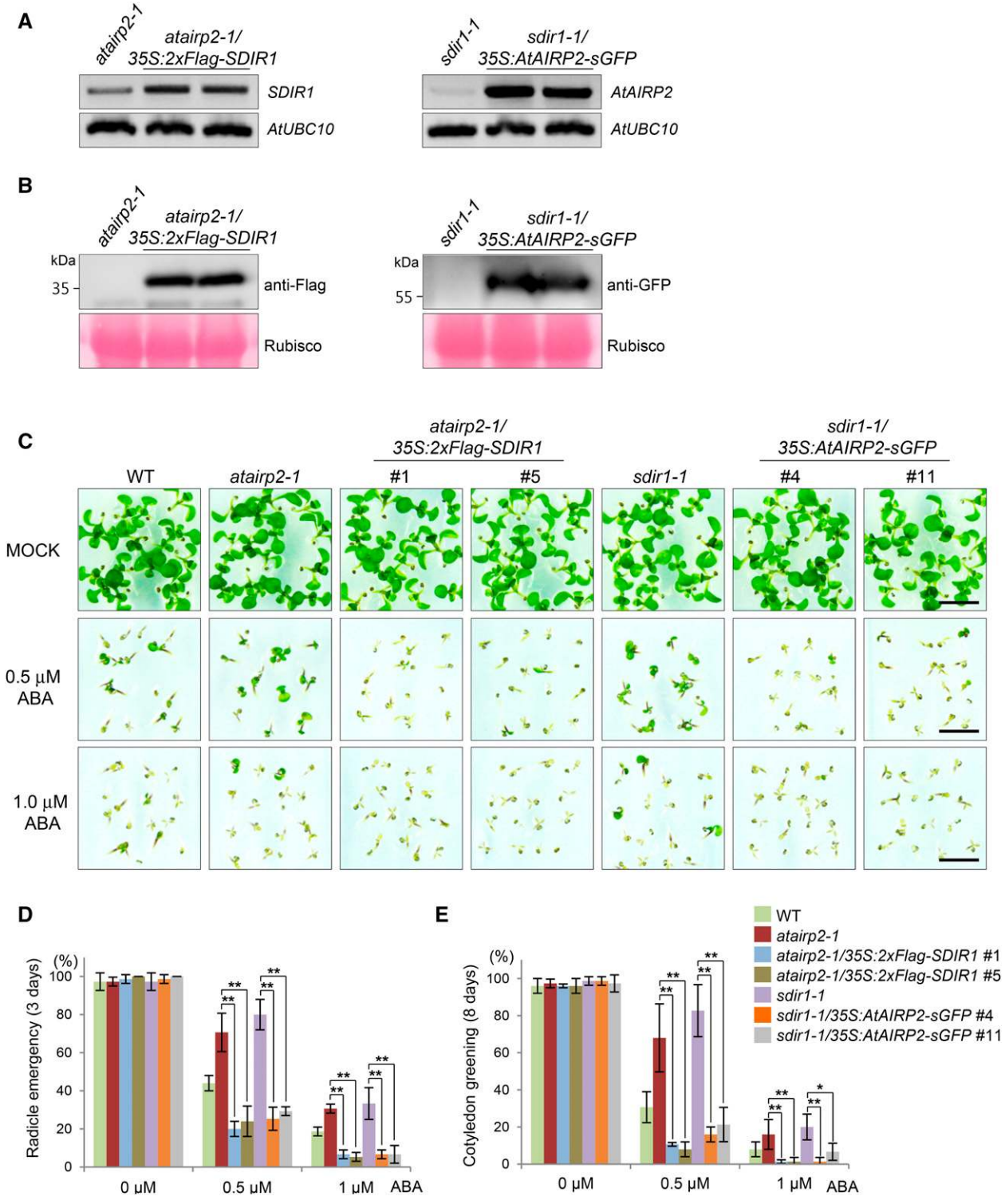


**Figure 5.** Reciprocal complementation assays of AtAIRP2 and SDIR1 RING E3 Ub ligases in ABA-mediated seed germination. A and B, RT-PCR (A) and immunoblot (B) analyses. *35S:AtAIRP2-sGFP* and *35S:2×Flag-SDIR1* were transformed into *sdir1-1* and *atairp2-1* mutants, respectively. Expression levels of *SDIR1* and *AtAIRP2* were examined in *atairp2-1/35S:2×Flag-SDIR1* (lines 1 and 5) and *sdir1-1/35S:AtARIP2* (lines 4 and 11) complementation T3 transgenic plants, respectively, by RT-PCR (A) and immunoblotting (B). *AtUBC10* and Rubisco large subunit were used as loading controls. C, Seed germination assays of *atairp2-1/35S:2×Flag-SDIR1* and *sdir1-1/35S:AtARIP2* complementation T3 transgenic plants in response to ABA. After imbibition in water for 2 d at 4°C, wild-type (WT), *atairp2-1* and *sdir1-1* mutant, and *atairp2-1/35S:2xFlag-SDIR1* and *sdir1-1/35S:AtAIRP2-sGFP* complementation seeds were incubated on MS medium in the presence of different concentrations (0, 0.5, and 1 $\mu$M) of ABA at

in the cytosolic spherical body, in which the signals of AtAIRP2-sGFP and ATP1/SDIRIP1-mRFP were closely merged (middle and right in Fig. 7A). This raised the possibility that AtAIRP2 and ATP1/SDIRIP1 are colocalized to the discrete cytosolic punctae-like structure in response to MG132 in tobacco leaf cells.

The interaction between AtAIRP2 and ATP1/SDIRIP1 was further investigated using a BiFC assay in the presence of MG132. The N-terminal (nYFP) and C-terminal (cYFP) regions of yellow fluorescent protein (YFP) were fused to the C termini of ATP1/SDIRIP1 and AtAIRP2, respectively. A reconstituted fluorescent signal was undetected in tobacco cells in which nYFP + AtAIRP2-cYFP or ATP1/SDIRIP1-nYFP + cYFP was transiently expressed (Fig. 7B). In contrast, when ATP1/SDIRIP1-nYFP + AtAIRP2-cYFP were coexpressed, a clear punctate fluorescent signal was detected (Fig. 7B). This cytosolic spherical body was somewhat reminiscent of the nucleus. However, the results of BiFC in the presence of NLS-mRFP, a nuclear marker protein, indicated that the spherical BiFC signal was not merged with, but in close proximity to, the nucleus (Fig. 7B). These results suggest that AtAIRP2 and ATP1/SDIRIP1 interact in the cytosolic punctate compartment that lies within the vicinity of the nucleus.

### Subunits of the 26S Proteasome Complex (RPN12a and RPT1) and Molecular Chaperones (HSP70 and HSP101) Were Colocalized to the Cytosolic Spherical Body in Which AtAIRP2 and ATP1/SDIRIP1 Interact

Punctae-like colocalization and interacting BiFC signals of AtAIRP2 and ATP1/SDIRIP1 were detected in the presence of MG132 that decreased proteasomal activity (Fig. 7). Thus, we speculated that the 26S proteasome complex and molecular chaperones are associated with these cytosolic spherical bodies. To test this possibility, a BiFC assay was carried out in the presence to RPN12a and RPT1, subunits of the 26S proteasome complex, and the molecular chaperones HSP70 and HSP101. The results showed that both RPN12a and RPT1 are colocalized to the BiFC spherical compartment (Fig. 8A). Furthermore, localization signals for HSP70 and HSP101 were closely merged with these punctate bodies (Fig. 8B). In contrast, none of the colocalized signals was detected in the nucleus. Taken together, the results of localization (Fig. 7) and the BiFC assay (Fig. 8) indicate that AtAIRP2 and ATP1/SDIRIP1 interact in the cytosolic spherical compartment of tobacco leaf cells, where the 26S proteasome complex and molecular chaperones are closely associated.

## DISCUSSION

AtAIRP2 was identified previously as a cytosolic RING-type E3 Ub ligase that positively regulates an ABA-mediated drought response (Cho et al., 2011). In this study, we report that the chloroplast/nucleus-localized ATP1/SDIRIP1 is a substrate protein of AtAIRP2 in response to ABA and high-salt stress during the germination stage. A specific interaction between AtAIRP2 and ATP1/SDIRIP1 was detected by yeast two-hybrid, in vitro pull-down, and in vivo co-IP assays (Fig. 1). In vitro and in planta ubiquitination of ATP1/SDIRIP1 by AtAIRP2 also was demonstrated (Fig. 1). Consistent with these results, the cellular amount of ATP1/SDIRIP1 was negatively regulated by AtAIRP2 in a 26S proteasome-dependent manner (Fig. 2). Genetic analysis of the *35S:ATP1/SDIRIP1-RNAi/atairp2* double mutant progeny showed that AtAIRP2 is epistatic to ATP1/SDIRIP1 in ABA-mediated seed germination (Fig. 3). Based on these results, we concluded that AtAIRP2 exerts its positive effect on ABA signaling by down-regulating ATP1/SDIRIP1 through a UPS-dependent pathway during Arabidopsis seed germination and a high-salinity response in early seedling growth.

The ABA-responsive transcription factor ABI5 is a positive regulator of ABA signaling. ABI5 is ubiquitinated by a RING-type KEEP ON GOING and cullin 4-based DWD hypersensitive to ABA1 (DWA1) and DWA2 E3 ligases (Lee et al., 2010; Liu and Stone, 2013; Yu et al., 2015). Thus, ABA signaling is negatively regulated by at least three E3 ligases via down-regulation of a common substrate, ABI5. This negative regulation of ABA signaling by multiple E3 ligases might help plants to fine-tune their responses to diverse environmental factors.

SDIR1 is an ER membrane-localized RING E3 ligase that positively regulates ABA-dependent seed germination and the salt stress response (Zhang et al., 2007, 2015). SDIR1 targets and down-regulates ATP1/SDIRIP1, which is a negative factor of ABI5. Thus, the ABA sensitivity of the germination stage is modulated by two different RING-type E3 ligases, cytosolic AtAIRP2 (Figs. 1–3) and ER membrane-bound SDIR1 (Zhang et al., 2015), through ubiquitination of a common substrate protein, ATP1/SDIRIP1. These results suggest that ubiquitination of a single target protein by multiple E3 ligases is operated not only in the negative feedback loop (Lee et al., 2010; Liu and Stone, 2013) but also in the positive regulation (Figs. 1–3; Zhang et al., 2015) of ABA signaling in the early stage of Arabidopsis growth.

Moreover, AtAIRP2 and SDIR1 complement reciprocally in terms of the degradation of ATP1/SDIRIP1 (Fig. 4) and ABA- and salt stress-modulated seed

**Figure 5.** (*Continued.*)
22°C under a 16-h-light/8-h-dark photoperiod. Bars = 0.5 cm. D and E, Germination percentages were measured with respect to radicle emergence 3 d after germination (D) and cotyledon greening 8 d after germination (E). Results are presented as means ± SD (*, $P < 0.05$ and **, $P < 0.01$, Student's *t* test) of three independent biological replicates ($n = 25$).

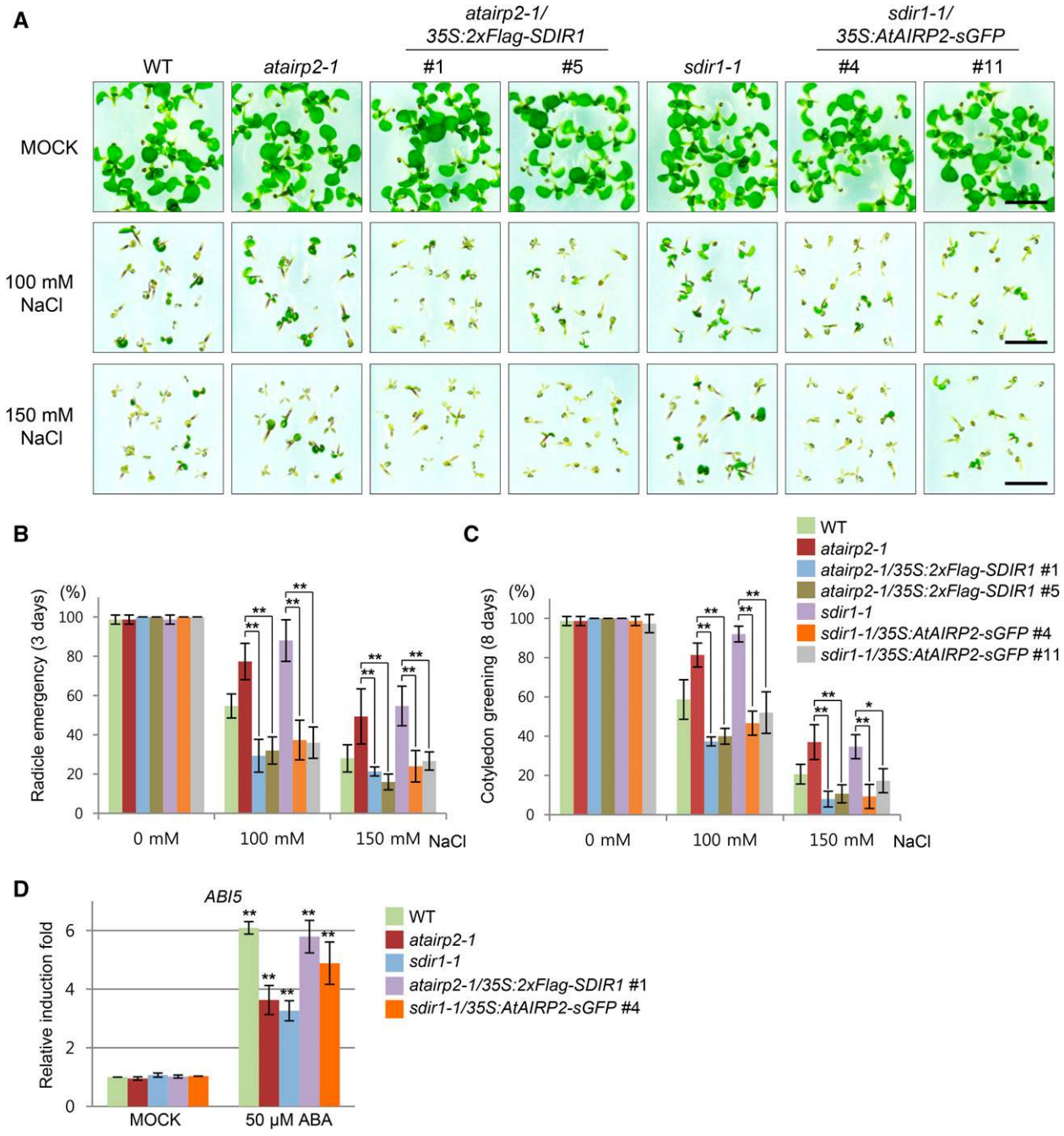


**Figure 6.** High-salinity responses of *atairp2-1/35S:2×Flag-SDIR1* and *sdir1-1/35S:AtARIP2* complementation T3 transgenic plants at the germination stage. A, Seed germination assays of *atairp2-1/35S:2×Flag-SDIR1* and *sdir1-1/35S:AtAIRP2-sGFP* complementation lines under high-salinity conditions. Wild-type (WT), *atairp2-1* and *sdir1-1* mutant, and *atairp2-1/35S:2×Flag-SDIR1* and *sdir1-1/35S:AtAIRP2-sGFP* complementation seeds were treated with different concentrations of NaCl (0, 100, and 150 mM) at 22°C under a 16-h-light/8-h-dark photoperiod. Bars = 0.5 cm. B and C, Germination percentages were evaluated in terms of radicle emergence 3 d after germination (B) and cotyledon greening 8 d after germination (C). Data represent means ± SD (*, $P < 0.05$ and **, $P < 0.01$, Student's *t* test) of three biological replicates ($n = 25$). D, Reciprocal qRT-PCR analysis of the ABA-responsive transcription factor *ABI5*. The *ABI5* transcript levels were examined in wild-type, *atairp2* and *sdir1* mutant, and *atairp2-1/35S:2×Flag-SDIR1* and *sdir1-1/35S:AtARIP2* complementation T3 transgenic plants by qRT-PCR. Arabidopsis glyceraldehyde-3-phosphate dehydrogenase was used as an internal control.

germination (Figs. 5 and 6). These combinatory actions of two different RING E3s might enhance the fitness of early seedlings, which are vulnerable to internal and external factors. It is worth noting that both AtAIRP2 and SDIR1 are positive factors in ABA-mediated stomatal closure and tolerance to drought (Zhang et al.,

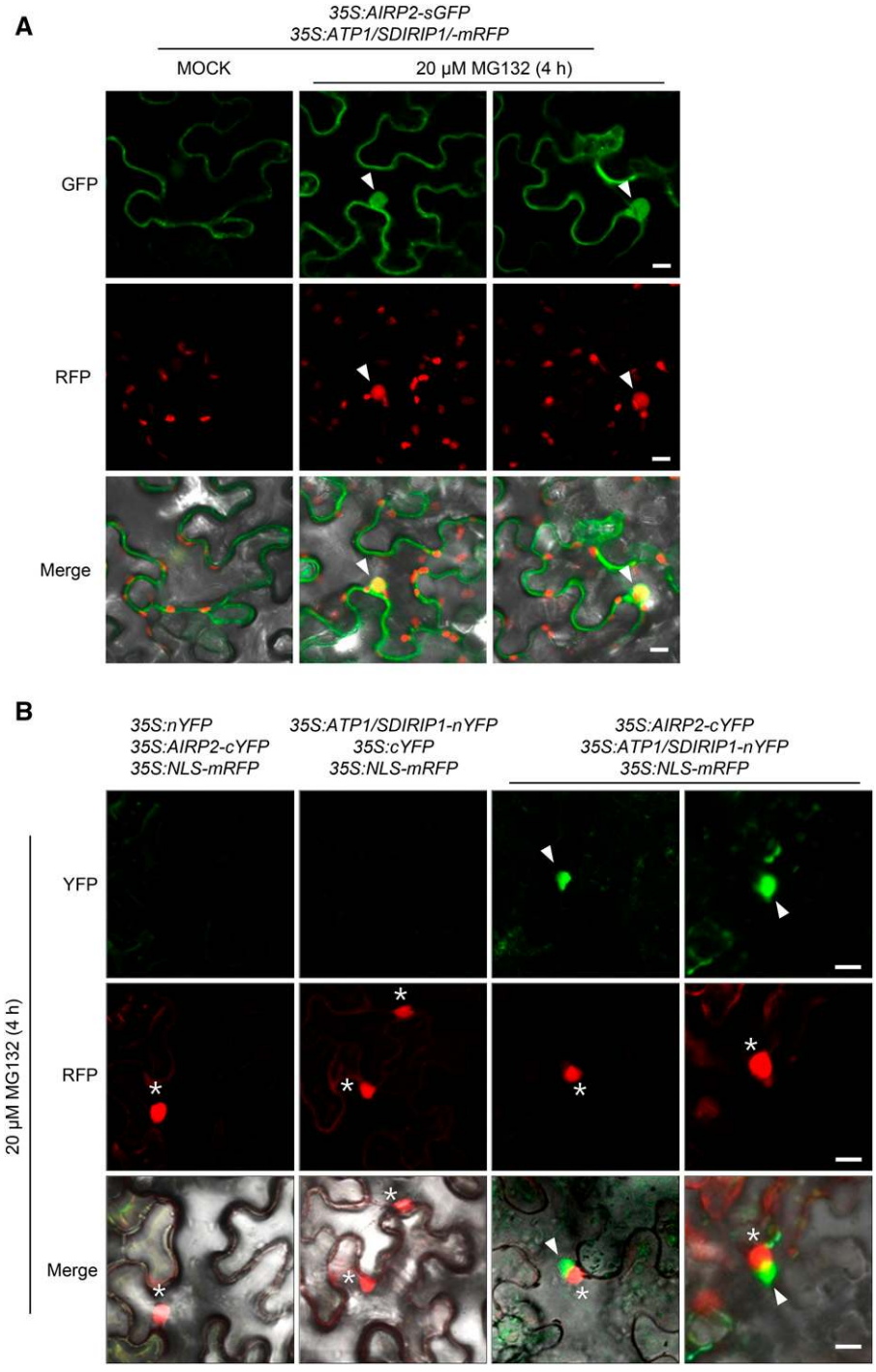


**Figure 7.** Subcellular localization and BiFC assays of AtAIRP2 and ATP1/SDIRIP1. A, Subcellular localization of AtAIRP2 and ATP1/SDIRIP1 in tobacco leaf epidermal cells. *35S:AtAIRP2-sGFP* and *35S:ATP1/SDIRIP1-mRFP* were introduced into tobacco epidermal cells by an *A. tumefaciens*-mediated transient expression method. After 2 d of incubation at 25°C under a 16-h-light/8-h-dark photoperiod, tobacco cells were treated with or without 20 $\mu$M MG132 for 4 h. The fluorescent signals from AtAIRP2-sGFP and ATP1/SDIRIP1-mRFP were detected via confocal microscopy. Arrowheads indicate cytosolic spherical bodies, in which colocalized signals of AtAIRP2-sGFP and ATP1/SDIRIP1-mRFP were detected. Bars = 10 $\mu$m. B, BiFC analysis of the in planta interaction between AtAIRP2 and ATP1/SDIRIP1. The full-length coding sequences of *ATP1/SDIRIP1* and *AtAIRP2* were fused to the N-terminal (nYFP) and C-terminal (cYFP) regions of YFP, respectively. The ATP1/SDIRIP1-nYFP + cYFP, AtAIRP2-cYFP + nYFP, and ATP1SDIRIP1-nYFP + AtAIRP2-cYFP proteins were coexpressed in tobacco leaf cells along with NLS-mRFP, a nuclear marker protein. After 2 d of incubation, tobacco cells were treated with 20 $\mu$M MG132 for 4 h. Reconstituted fluorescent signals were visualized by confocal microscopy. The arrowheads indicate BiFC signals from the interaction between ATP1/SDIRIP1-nYFP and AtAIRP2-cYFP, and the asterisks indicate nuclei. Bars = 10 $\mu$m.

2007; Cho et al., 2011). In contrast, up- and down-regulation of ATP1/SDIRIP1 have negligible effects on ABA signaling in the drought stress response (Zhang et al., 2015), suggesting that the negative action of ATP1/SDIRIP1 is specific to the germination stage. Under normal growth conditions, *AtAIRP2* is expressed in the vascular tissues of early seedlings, whereas *SDIR1* is expressed predominantly in root tissues (Zhang et al., 2007; Cho et al., 2011). However, both *AtAIRP2* and *SDIR1* are highly induced by dehydration stress in guard cells. Thus, it is still unknown whether AtAIRP2 and SDIR1 share a common target protein(s) and whether their modes of action are combinatory or independent in the ABA-dependent drought tolerance response during postgermination growth.

In mammalian systems, PCD plays dual roles as an enzyme for the regeneration of oxidized pterin cofactors in the process of aromatic amino acid metabolism

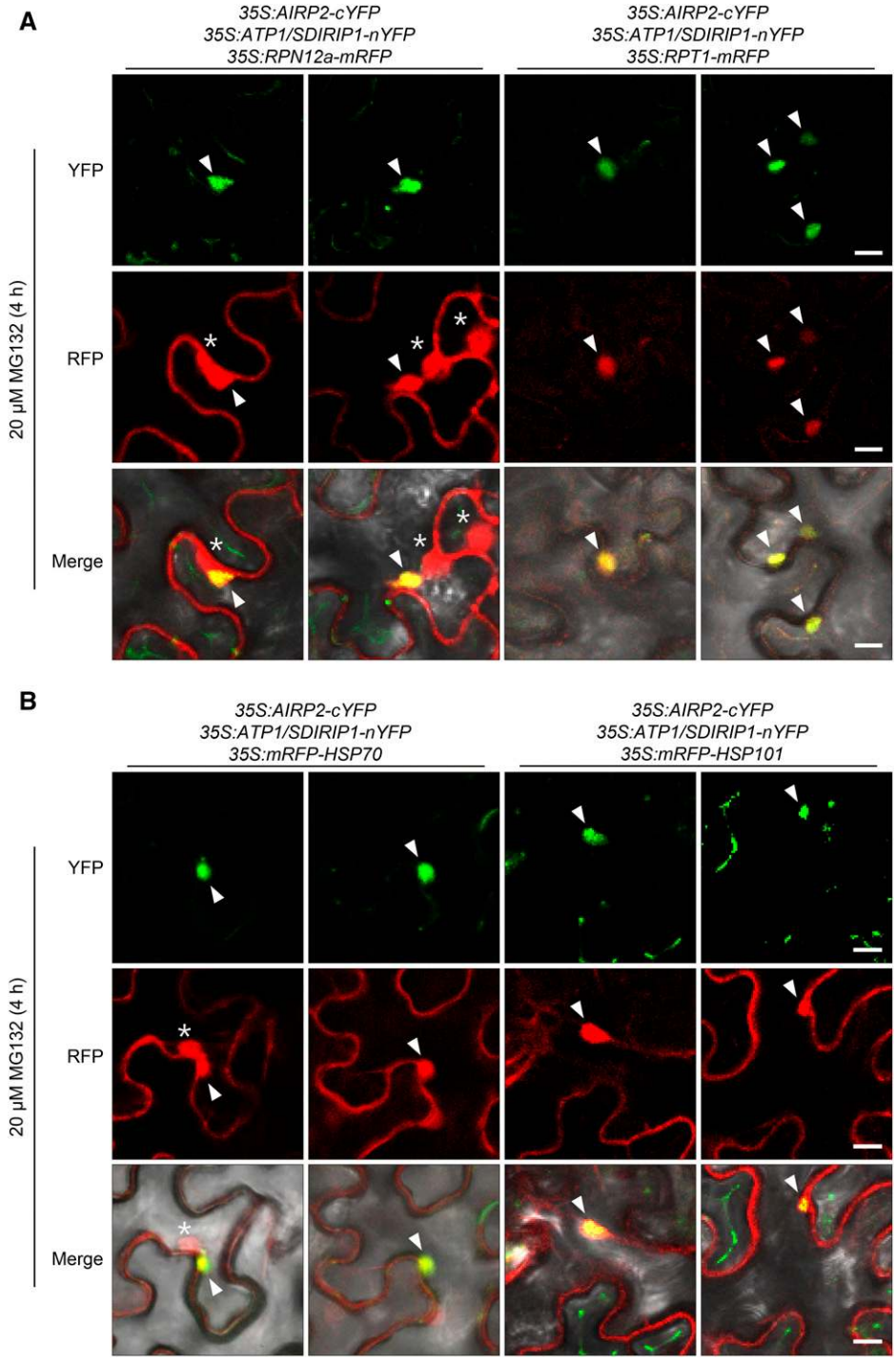


**Figure 8.** Colocalization of the 26S proteasome subunits (RPN12a and RPT1) and molecular chaperones (HSP70 and HSP101) to the cytosolic spherical compartment. A, ATP1/SDIRIP1-nYFP + AtAIRP2-cYFP proteins were coexpressed with RPN12a-mRFP (left) or RPT1-mRFP (right) in tobacco leaf cells in the presence of 20 $\mu$M MG132. The fluorescent signals from YFP and mRFP were detected using confocal microscopy. The arrowheads indicate cytosolic spherical bodies, in which AtAIRP2, ATP1/SDIRIP1, RPN12a, and RPT1 proteins are colocalized, and the asterisks indicate nuclei. Bars = 10 $\mu$m. B, ATP1/SDIRIP1-nYFP + AtAIRP2-cYFP proteins were coexpressed with mRFP-HSP70 (left) or mRFP-HSP101 (right) in tobacco leaf cells in the presence of 20 $\mu$M MG132. Bars = 10 $\mu$m.



and as a nuclear transcription cofactor (Suck and Ficner, 1996). ATP1/SDIRIP1 was identified as a chloroplast-localized Arabidopsis homolog of PCD without enzyme activity (Naponelli et al., 2008). Zhang et al. (2015) found that ATP1/SDIRIP1 also is localized to the nucleus and cell periphery in addition to chloroplasts. They further reported that SDIR1 and ATP1/SDIRIP1 interact on the cytosolic side of the ER outer membrane. Under our experimental conditions, AtAIRP2 was present in the cytosolic fraction, whereas ATP1/SDIRIP1 was localized predominantly to the chloroplasts of tobacco leaf epidermal cells (Fig. 7A), which indicates that AtAIRP2 and ATP1/SDIRIP1 do not exhibit a detectable colocalization pattern under normal conditions. However, when the activity of the 26S proteasome complex was inhibited by MG132, colocalization and interacting signals of AtAIRP2 and ATP1/SDIRIP1 appeared in the cytosolic spherical

body of tobacco leaf cells, in which proteasome subunits (RPN12a and RPT1) and molecular chaperones (HSP70 and HSP101) were colocalized (Figs. 7 and 8). In many cases, if not all, this punctate compartment was observed in close proximity to the nucleus.

In yeast and mammalian cells, aggregated and misfolded cytotoxic proteins are sequestered in the protein quality control (PQC) compartments. Aggresome, juxtanuclear quality control (JUNQ), insoluble protein deposit (IPOD), and ER-associated compartment are four types of PQC bodies (Johnston et al., 1998; Arrasate et al., 2004; Bagola and Sommer, 2008; Kaganovich et al., 2008). Molecular chaperones and the 26S proteasome complex are colocalized to these PQC bodies. Proteasome impairment and high-temperature conditions have been shown to lead to the increased formation of two punctae-like cytosolic compartments, JUNQ and IPOD (Kaganovich et al., 2008). Soluble ubiquitinated misfolded proteins are prone to be sorted to JUNQ, whereas nonubiquitinated aggregated proteins accumulate in IPOD, in which ATG8a, a key component of autophagy, is colocalized (Bagola and Sommer, 2008; Kaganovich et al., 2008). Active turnover of misfolded proteins occurs in these PQC bodies, suggesting that the PQC compartments are not passive by-products of protein aggregation but rather serve an important quality-control function in mammalian cells (Weisberg et al., 2012; Ogrodnik et al., 2014; Zaarur et al., 2014). Unlike autophagy, which diminishes unnecessary toxic cellular components through an irreversible pathway, relocation of soluble misfolded and ubiquitinated proteins from the JUNQ body to the cytosolic fraction has been reported in yeast cells (Kaganovich et al., 2008). In human HEK cells, large JUNQ inclusion bodies often are detected in nearly every cell. On the other hand, in human N2a and CHO cells, the JUNQ structure is less apparent under normal conditions, but inhibition of the proteasome complex leads to the appearance of visible JUNQs (Ogrodnik et al., 2014). Thus, it is likely that the formation of JUNQ differs in different cell types and is dependent on the cellular levels of misfolded proteins (Ogrodnik et al., 2014). In tobacco cells, the cytosolic spherical compartment containing AtAIRP2 and ATP1/SDIRIP1 was detected in proximity to the nucleus after the inhibition of proteasome activity in tobacco cells, which is somewhat reminiscent of the mammalian JUNQ bodies (Figs. 7 and 8). It is of interest that *AtAIRP2* and its two homologs, *At3g47160* and *At5g58787* (both of which have 64% identity to *AtAIRP2*), are up-regulated by high-temperature treatment that increases the accumulation of misfolded proteins and the formation of JUNQ (Kaganovich et al., 2008; Supplemental Fig. S3). At present, however, it remains to be clarified whether the cytosolic spherical body is a JUNQ-like PQC compartment in tobacco cells.

Because (1) the cytosolic spherical structure, in which AtAIRP2 and ATP1/SDIRIP1 interact with each other, appeared after the inhibition of the proteasome complex and (2) the proteasome subunits and heat shock proteins were closely associated with this punctate compartment, we propose that, in response to ABA and high-salt stress, ATP1/SDIRIP1 is ubiquitinated by AtAIRP2 in the cytosolic fraction and then rapidly degraded by the 26S proteasome before ATP1/SDIRIP1 enters the chloroplasts and/or nucleus (Fig. 9). Furthermore, ATP1/SDIRIP1 is ubiquitinated by SDIR1 on the cytosolic side of the ER membrane (Fig. 9). This rapid down-regulation of ATP1/SDIRIP1 by the

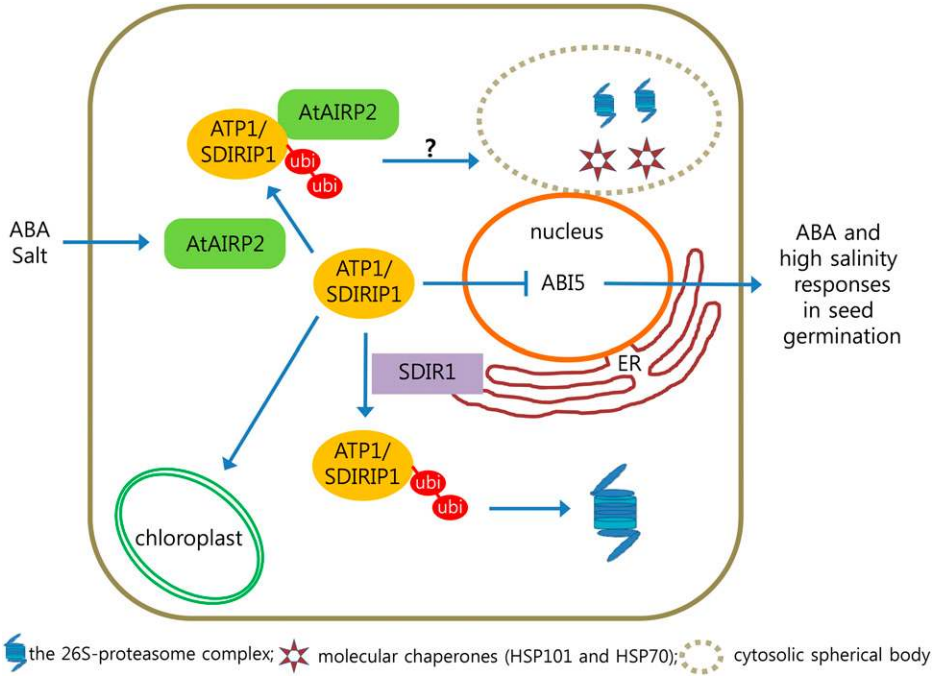


**Figure 9.** Working model of AtAIRP2 and SDIR RING E3 Ub ligases in ABA and high-salinity responses during seed germination. In response to ABA and high-salt stress, ATP1/SDIRIP1 is ubiquitinated by AtAIRP2 in the cytosol and then rapidly degraded by the 26S proteasome complex before ATP1/SDIRIP1 enters the chloroplasts and/or nucleus. In addition, ATP1/SDIRIP1 is ubiquitinated by SDIR1 on the cytosolic side of the ER membrane (Zhang et al., 2015). The proteasome-dependent down-regulation of ATP1/SDIRIP1 by the combinatorial actions of two RING-type E3 Ub ligases results in the increased response to ABA and high salinity in the germination stage. The possible role of the cytosolic spherical body in the interaction of AtAIRP2 and ATP1/SDIRIP1 remains to be determined.

concomitant actions of two RING E3 Ub ligases results in the increased responses toward ABA and high salinity during the germination stage. Although ATP1/SDIRIP1 down-regulates *ABI5* expression in the nucleus, its role in the chloroplast is still unknown (Zhang et al., 2015). In conclusion, our data suggest that AtAIRP2 plays a positive role in response to ABA and high-salinity stress during germination growth via the UPS-dependent down-regulation of ATP1/SDIRIP1 in Arabidopsis.

## MATERIALS AND METHODS

### Plant Materials and Growth Conditions

Arabidopsis (*Arabidopsis thaliana* Columbia-0) wild-type and *sdir1-1* (SALK_114361) mutant seeds were obtained from the Arabidopsis Biological Resource Center. The generation of *35S:AtAIRP2-sGFP* transgenic and *atairp2-1* mutant plants was described in a previous study (Cho et al., 2011). The *35S:ATP1/SDIRIP1-RNAi* knockdown and *35S:2×Flag-SDIR1*- and *35S:ATP1/SDIRIP1-3×Myc*-overexpressing transgenic plants were constructed by means of the *Agrobacterium tumefaciens*-mediated transformation method (Clough and Bent, 1998). The insertion and expression of transgenes were examined by genotyping PCR and RT-PCR, respectively. Expression levels of 2×Flag-SDIR1 and ATP1/SDIRIP1-3×Myc recombinant proteins were inspected via immunoblot assays using anti-Flag (Sigma-Aldrich) and anti-Myc (Applied Biological Materials) antibodies, respectively, as described previously (Kim et al., 2016). For reciprocal complementation assays, *35S:2×Flag-SDIR1*-and *35S:AtAIRP2-sGFP*-overexpressing transgenic plants were crossed with T-DNA-inserted *atairp2-1* and *sdir1-1* knockout mutant lines, respectively. The *35S:ATP1/SDIRIP1-RNAi/atairp2* double mutant progeny were generated by crossing *35S:ATP1/SDIRIP1-RNAi* and *atairp2* single mutant plants. Plants used in this study were grown at 22°C under long-day growth conditions (16 h of light/8 h of dark).

### Vector Construction

To generate the *35S:ATP1/SDIRIP1-RNAi* knockdown plants, a partial region of *ATP1/SDIRIP1* cDNA (from 650 to 870 bp) was amplified with a gene-specific primer set (Supplemental Table S1), and the PCR product was ligated into the pENTR vector harboring a GUS intron sequence. The *RNAi* construct was confirmed by DNA sequencing and subcloned into the pEG100 binary vector using LR Clonase II (Thermo Fisher Scientific). *SDIR1* and *ATP1/SDIRIP1* coding sequences were amplified by PCR with respective gene-specific primers. The PCR products were ligated into the *pENTR-2×Flag* and *pENTR-3×Myc* vectors, and the ENTR clones were subcloned into a pEG100 binary vector using LR Clonase. The binary vectors were transformed into *A. tumefaciens* strain GV3101 via the freeze-thaw transformation method (Weigel and Glazebrook, 2006). For subcellular localization assays, full-length coding regions of *HSP70*, *HSP101*, *RPN12a*, and *RPT1* were ligated into the pENTR-mRFP plasmid and then subcloned into the pEG100 vector. For in vitro ubiquitination and cell-free degradation assays, a full-length coding region of *ATP1/SDIRIP1* was ligated into the pProex hta vector, which contains in-frame 3×HA or 6×Myc tag sequences. The DNA sequences of the primers used in this study are shown in Supplemental Table S1.

### Yeast Two-Hybrid Assays

The yeast two-hybrid and transformation method used in this study was described by Kim and Kim (2013). Briefly, the pGBKT7-AtAIRP2 plasmid was cotransformed into *Saccharomyces cerevisiae* strain AH109 (Clontech) with an Arabidopsis two-hybrid cDNA library. The cells were incubated for 3 d on SD/-Trp/-Leu/-His or SD/-Trp/-Leu/-His/-Ade growth medium at 30°C. p53 (murine $p53^{72\text{-}390}$) + T-antigen was used as a positive control, whereas lambda (human lamin $C^{66\text{-}230}$) + T-antigen was used as a negative control.

### Recombinant Protein Expression and Purification

Bacterially expressed MBP, MBP-AtAIRP2, and MBP-$AtAIRP2^{H163A}$ recombinant proteins were purified as described in a previous study (Seo et al., 2016). The 6×His-tagged recombinant proteins (6×His-3×HA-ATP1/SDIRIP1, 6×His-ATP1/SDIRIP1-6×Myc, and 6×His-RGA1-2×Flag) were purified using Ni-NTA resin according to the manufacturer's protocol (Qiagen).

### In Vitro Pull-Down and in Vivo Co-IP Experiments

An in vitro pull-down assay was carried out as described by Cho et al. (2008) with slight modifications. Purified 6×His-3×HA-ATP1/SDIRIP1 recombinant protein (500 ng) was incubated with MBP or MBP-AtAIRP2 (1 $\mu$g) in the presence of an amylose resin (Qiagen) in pull-down buffer (1× PBS, 25 mM EDTA, 1 mM PMSF, protease inhibitor cocktail VI [AG Scientific], and 0.5% Triton X-100) for 2 h at 4°C with gentle rotation. The incubated resin was washed three times with pull-down buffer, and the resin-bound proteins were eluted with 2× SDS sample buffer. The eluted proteins were analyzed via immunoblot analysis.

An in vivo co-IP assay was performed using the protocol described by Son et al. (2010). *A. tumefaciens* cells harboring the *35S:p19*, *35S:ATP1/SDIRIP1-3×Myc*, or *35S:2×Flag-AtAIRP2* construct were infiltrated into tobacco (*Nicotiana benthamiana*) leaves and incubated for 48 h. An equal amount of soluble extract (20 $\mu$g of total proteins) was prepared from leaves and incubated for 2 h in the presence of anti-Flag M2 affinity resin (Sigma-Aldrich). After extensive washing, bound proteins were eluted from the affinity resin with 0.1 M Gly-HCl buffer, pH 2.3. The eluted proteins were examined by immunoblot analysis.

### Cell-Free Degradation and in Vitro Ubiquitination Assays

Soluble crude extracts (phosphate-buffered saline, 10 mM $MgCl_2$, and 25% glycerol) were prepared from wild-type, *atairp2*, and *35S:AtAIRP2-sGFP* leaves. Leaf crude extract (10 $\mu$g of total proteins) was incubated with 6×His-ATP1/SDIRIP1-6×Myc (500 ng) and 6×His-RGA1-2×Flag (500 ng) recombinant proteins for 0.5, 1, and 2 h in the presence or absence of 50 $\mu$M MG132 (AG Scientific). The reaction was stopped by adding 2× SDS sample buffer and examined by immunoblot analysis using anti-Myc (Applied Biological Materials) and anti-Flag (Sigma-Aldrich) antibodies. The intensity of protein bands was quantified by ImageJ software (https://imagej.nih.gov/).

For the in vitro ubiquitination assay, purified 6×His-ATP1/SDIRIP1-6×Myc (500 ng) was incubated in the presence or absence of E1 (AtUBA1; 200 ng), E2 (AtUBC8; 200 ng), E3 (MBP-AtAIRP2 or MBP-$AtAIRP2^{H163A}$; 500 ng), and Ub (10 $\mu$g; Enzo Lifescience) at 30°C for 1 h as described by Lee et al. (2009). The reaction mixture was inspected via immunoblotting with anti-Myc antibody or was immunoprecipitated using anti-HA resin (Roche). The eluted protein was resolved via SDS-PAGE, and the ubiquitinated proteins were visualized by immunoblotting with anti-Ub antibody (Santa Cruz).

### Protoplast Cotransfection Assay

Isolation and transfection of Arabidopsis leaf protoplasts were performed as described by Yoo et al. (2007). The plasmids (CsCl-gradient maxiprep scale) that contained *35S:AtAIRP2-sGFP*, *35S:ATP1/SDIRIP1-3×Myc*, and *35S:DSred2* constructs were transfected into isolated protoplasts and incubated for 16 h with or without 50 $\mu$M MG132. Protein expression levels in the protoplasts were detected by immunoblotting with anti-GFP (Clontech), anti-Myc (Applied Biological Materials), and anti-DSred2 (Clontech) antibodies. Cotransfection efficiency was calculated to be 91.9% by counting the fluorescent signals of coexpressed sGFP and mRFP (Supplemental Fig. S4).

### Germination Assay

Germination assays were conducted as described by Hwang et al. (2015). Briefly, freshly harvested Arabidopsis seeds were treated with 30% bleach solution and then washed 10 times with sterilized distilled water. After imbibition at 4°C for 48 h, the seeds were germinated in MS medium supplemented with 1% Suc and 0.8% agarose for 8 d in the presence or absence of exogenous ABA (0.5 and 1 $\mu$M) or NaCl (100 and 150 mM). Percentages of radicle emergence and cotyledon greening were counted at 3 and 8 d after sowing, respectively.

### Protein Expression in Tobacco Leaf Cells and Microscopy

*A. tumefaciens* cells harboring the *35S:AtAITP2-sGFP* or *35S:ATP1/SDIRIP1-mRFP* construct were grown in YEP medium (1% yeast extract, 1% peptone, and 0.5% NaCl, pH 7.5) at 28°C for 12 h and harvested by centrifugation. Harvested

cells were resuspended in infiltration medium (10 mM MES, pH 5.7, 10 mM $MgCl_2$, and 0.5 mM acetosyringone [MB Cell]). An equal amount of harvested cells was then infiltrated into 2-week-old tobacco leaves as described by Sparkes et al. (2006). After 48 to 72 h of incubation, the transiently expressed GFP and RFP fluorescence signals were visualized by confocal microscopy (LSM880 META; Carl Zeiss).

## BiFC

The full-length coding region of *ATP1/SDIRIP1* was introduced into the pENTR-nYFP vector containing the N-terminal region of YFP (amino acids 1–174). *AtAIRP2* was ligated to the pENTR-cYFP plasmid that contained the C-terminal region of YFP (amino acids 175–237). *A. tumefaciens* strain GV3101 harboring the nYFP- and cYFP-fused constructs was coinfiltrated into tobacco leaves as described by Seo et al. (2016) and incubated for 3 d. Reconstituted fluorescent signals in the infiltrated leaf cells were visualized by confocal microscopy. *35S:nYFP + 35S:cYFP* was used as a negative control. *35S:bZIP63-nYFP + 35S:bZIP63-cYFP*, which results in the formation of a homodimeric complex, was used as a positive control (Supplemental Fig. S5).

## Immunoblot Analysis

Protein samples were resolved by SDS-PAGE and transferred to polyvinylidene difluoride membranes (Millipore). Transferred proteins were probed with anti-Ub (1:5,000 dilution), anti-HA (1:5,000 dilution), anti-Flag (1:5,000 dilution), anti-GFP (1:2,500 dilution), anti-DsRed2 (1:2,000 dilution), and anti-Myc (1:5,000 dilution) antibodies. Horseradish peroxidase-conjugated anti-mouse (1:10,000 dilution; Millipore) and anti-rabbit (1:10,000 dilution; Applied Biological Materials) antibodies were used as secondary antibodies for detecting signals.

## RT-PCR

Extraction of total RNA was performed using the Easy Spin II plant total RNA extraction kit (Intron) in accordance with the manufacturer's protocol. Total RNA (2 $\mu$g) and a Topscript cDNA synthesis kit (Enzynomics) were used for the RT reaction. A detailed protocol for the RT-PCR performed in this study was described previously (Seo et al., 2012).

## Amino Acid Sequence Alignment

The deduced amino acid sequences of AtAIRP2 and its homologs At3g47160 and At5g58787 were aligned using ClustalX2.0 software (http://www.clustal.org) and further edited using Genedoc software (http://www.nrbsc.org/gfx/genedoc/).

## Accession Numbers

Sequence data from this article can be found in the GenBank/EMBL data libraries under accession numbers *AtAIRP2* (At5g01520), *SDIR1* (At3g55530), *ATP1/SDIRIP1* (At5g51110), *RPN12a* (At1g64520), *RPT1* (At3g45780), *HSP70* (At3g12580), and *HSP101* (At1g74310).

## Supplemental Data

The following supplemental materials are available.

**Supplemental Figure S1.** RT-PCR analysis of *ATP1/SDIRIP1-RNAi* knockdown T3 transgenic plants.

**Supplemental Figure S2.** RT-PCR analysis of *35S:ATP1/SDIRIP1-RNAi/atairp2* double mutant alleles.

**Supplemental Figure S3.** Sequence analysis and heat shock induction of *AtAIRP2* and its two homologs.

**Supplemental Figure S4.** Arabidopsis protoplast cotransfection efficiency test.

**Supplemental Figure S5.** The BiFC test experiment.

**Supplemental Table S1.** PCR primer sequences used for this article.

## ACKNOWLEDGMENT

We thank Dr. Ho Seok Lee for providing tobacco plants.

Received April 6, 2017; accepted June 13, 2017; published June 16, 2017.

## LITERATURE CITED

**Arrasate M, Mitra S, Schweitzer ES, Segal MR, Finkbeiner S** (2004) Inclusion body formation reduces levels of mutant huntingtin and the risk of neuronal death. Nature **431:** 805–810

**Bagola K, Sommer T** (2008) Protein quality control: on IPODs and other JUNQ. Curr Biol **18:** R1019–R1021

**Bu Q, Li H, Zhao Q, Jiang H, Zhai Q, Zhang J, Wu X, Sun J, Xie Q, Wang D, et al** (2009) The Arabidopsis RING finger E3 ligase RHA2a is a novel positive regulator of abscisic acid signaling during seed germination and early seedling development. Plant Physiol **150:** 463–481

**Cheng MC, Hsieh EJ, Chen JH, Chen HY, Lin TP** (2012) Arabidopsis RGLG2, functioning as a RING E3 ligase, interacts with AtERF53 and negatively regulates the plant drought stress response. Plant Physiol **158:** 363–375

**Cho SK, Ryu MY, Seo DH, Kang BG, Kim WT** (2011) The Arabidopsis RING E3 ubiquitin ligase AtAIRP2 plays combinatory roles with AtAIRP1 in abscisic acid-mediated drought stress responses. Plant Physiol **157:** 2240–2257

**Cho SK, Ryu MY, Song C, Kwak JM, Kim WT** (2008) Arabidopsis PUB22 and PUB23 are homologous U-box E3 ubiquitin ligases that play combinatory roles in response to drought stress. Plant Cell **20:** 1899–1914

**Clough SJ, Bent AF** (1998) Floral dip: a simplified method for Agrobacterium-mediated transformation of *Arabidopsis thaliana*. Plant J **16:** 735–743

**Cutler SR, Rodriguez PL, Finkelstein RR, Abrams SR** (2010) Abscisic acid: emergence of a core signaling network. Annu Rev Plant Biol **61:** 651–679

**Dill A, Thomas SG, Hu J, Steber CM, Sun TP** (2004) The *Arabidopsis* F-box protein SLEEPY1 targets gibberellin signaling repressors for gibberellin-induced degradation. Plant Cell **16:** 1392–1405

**Dreher K, Callis J** (2007) Ubiquitin, hormones and biotic stress in plants. Ann Bot (Lond) **99:** 787–822

**Finkelstein RR, Gampala SS, Rock CD** (2002) Abscisic acid signaling in seeds and seedlings. Plant Cell (Suppl) **14:** S15–S45

**Gomez-Cadenas A, Vives V, Zandalinas SI, Manzi M, Sanchez-Perez AM, Perez-Clemente RM, Arbona V** (2015) Abscisic acid: a versatile phytohormone in plant signaling and beyond. Curr Protein Pept Sci **16:** 413–434

**Guerra DD, Callis J** (2012) Ubiquitin on the move: the ubiquitin modification system plays diverse roles in the regulation of endoplasmic reticulum- and plasma membrane-localized proteins. Plant Physiol **160:** 56–64

**Hwang JH, Seo DH, Kang BG, Kwak JM, Kim WT** (2015) Suppression of Arabidopsis AtPUB30 resulted in increased tolerance to salt stress during germination. Plant Cell Rep **34:** 277–289

**Johnston JA, Ward CL, Kopito RR** (1998) Aggresomes: a cellular response to misfolded proteins. J Cell Biol **143:** 1883–1898

**Kaganovich D, Kopito R, Frydman J** (2008) Misfolded proteins partition between two distinct quality control compartments. Nature **454:** 1088–1095

**Kim EY, Park KY, Seo YS, Kim WT** (2016) Arabidopsis small rubber particle protein homolog SRPs play dual roles as positive factors for tissue growth and development and in drought stress responses. Plant Physiol **170:** 2494–2510

**Kim JH, Kim WT** (2013a) The Arabidopsis RING E3 ubiquitin ligase AtAIRP3/LOG2 participates in positive regulation of high-salt and drought stress responses. Plant Physiol **162:** 1733–1749

**Kim SJ, Kim WT** (2013b) Suppression of Arabidopsis RING E3 ubiquitin ligase AtATL78 increases tolerance to cold stress and decreases tolerance to drought stress. FEBS Lett **587:** 2584–2590

**Kim SJ, Ryu MY, Kim WT** (2012) Suppression of Arabidopsis RING-DUF1117 E3 ubiquitin ligases, AtRDUF1 and AtRDUF2, reduces tolerance to ABA-mediated drought stress. Biochem Biophys Res Commun **420:** 141–147

**Kim TH** (2014) Mechanism of ABA signal transduction: agricultural highlights for improving drought tolerance. J Plant Biol **57:** 1–8

**Kleiger G, Mayor T** (2014) Perilous journey: a tour of the ubiquitin-proteasome system. Trends Cell Biol **24:** 352–359

**Kraft E, Stone SL, Ma L, Su N, Gao Y, Lau OS, Deng XW, Callis J** (2005) Genome analysis and functional characterization of the E2 and RING-type E3 ligase ubiquitination enzymes of Arabidopsis. Plant Physiol **139:** 1597–1611

**Lee HK, Cho SK, Son O, Xu Z, Hwang I, Kim WT** (2009) Drought stress-induced Rma1H1, a RING membrane-anchor E3 ubiquitin ligase homolog, regulates aquaporin levels via ubiquitination in transgenic *Arabidopsis* plants. Plant Cell **21:** 622–641

**Lee JH, Kim WT** (2011) Regulation of abiotic stress signal transduction by E3 ubiquitin ligases in Arabidopsis. Mol Cells **31:** 201–208

**Lee JH, Yoon HJ, Terzaghi W, Martinez C, Dai M, Li J, Byun MO, Deng XW** (2010) DWA1 and DWA2, two *Arabidopsis* DWD protein components of CUL4-based E3 ligases, act together as negative regulators in ABA signal transduction. Plant Cell **22:** 1716–1732

**Li H, Jiang H, Bu Q, Zhao Q, Sun J, Xie Q, Li C** (2011) The Arabidopsis RING finger E3 ligase RHA2b acts additively with RHA2a in regulating abscisic acid signaling and drought response. Plant Physiol **156:** 550–563

**Liu H, Stone SL** (2013) Cytoplasmic degradation of the Arabidopsis transcription factor abscisic acid insensitive 5 is mediated by the RING-type E3 ligase KEEP ON GOING. J Biol Chem **288:** 20267–20279

**Lyzenga WJ, Stone SL** (2012) Abiotic stress tolerance mediated by protein ubiquitination. J Exp Bot **63:** 599–616

**Mehrotra R, Bhalothia P, Bansal P, Basantani MK, Bharti V, Mehrotra S** (2014) Abscisic acid and abiotic stress tolerance: different tiers of regulation. J Plant Physiol **171:** 486–496

**Naponelli V, Noiriel A, Ziemak MJ, Beverley SM, Lye LF, Plume AM, Botella JR, Loizeau K, Ravanel S, Rébeillé F, et al** (2008) Phylogenomic and functional analysis of pterin-4a-carbinolamine dehydratase family (COG2154) proteins in plants and microorganisms. Plant Physiol **146:** 1515–1527

**Ogrodnik M, Salmonowicz H, Brown R, Turkowska J, Średniawa W, Pattabiraman S, Amen T, Abraham AC, Eichler N, Lyakhovetsky R, et al** (2014) Dynamic JUNQ inclusion bodies are asymmetrically inherited in mammalian cell lines through the asymmetric partitioning of vimentin. Proc Natl Acad Sci USA **111:** 8049–8054

**Park SY, Fung P, Nishimura N, Jensen DR, Fujii H, Zhao Y, Lumba S, Santiago J, Rodrigues A, Chow TF, et al** (2009) Abscisic acid inhibits type 2C protein phosphatases via the PYR/PYL family of START proteins. Science **324:** 1068–1071

**Pratelli R, Guerra DD, Yu S, Wogulis M, Kraft E, Frommer WB, Callis J, Pilot G** (2012) The ubiquitin E3 ligase LOSS OF GDU2 is required for GLUTAMINE DUMPER1-induced amino acid secretion in Arabidopsis. Plant Physiol **158:** 1628–1642

**Qin F, Sakuma Y, Tran LS, Maruyama K, Kidokoro S, Fujita Y, Fujita M, Umezawa T, Sawano Y, Miyazono K, et al** (2008) *Arabidopsis* DREB2A-interacting proteins function as RING E3 ligases and negatively regulate plant drought stress-responsive gene expression. Plant Cell **20:** 1693–1707

**Rodrigues A, Adamo M, Crozet P, Margalha L, Confraria A, Martinho C, Elias A, Rabissi A, Lumbreras V, González-Guzmán M, et al** (2013) ABI1 and PP2CA phosphatases are negative regulators of Snf1-related protein kinase1 signaling in *Arabidopsis*. Plant Cell **25:** 3871–3884

**Ryu MY, Cho SK, Kim WT** (2010) The Arabidopsis C3H2C3-type RING E3 ubiquitin ligase AtAIRP1 is a positive regulator of an abscisic acid-dependent response to drought stress. Plant Physiol **154:** 1983–1997

**Sadanandom A, Bailey M, Ewan R, Lee J, Nelis S** (2012) The ubiquitin-proteasome system: central modifier of plant signalling. New Phytol **196:** 13–28

**Seo DH, Ahn MY, Park KY, Kim EY, Kim WT** (2016) The N-terminal UND motif of the *Arabidopsis* U-box E3 ligase PUB18 is critical for the negative regulation of ABA-mediated stomatal movement and determines its ubiquitination specificity for exocyst subunit Exo70B1. Plant Cell **28:** 2952–2973

**Seo DH, Ryu MY, Jammes F, Hwang JH, Turek M, Kang BG, Kwak JM, Kim WT** (2012) Roles of four Arabidopsis U-box E3 ubiquitin ligases in negative regulation of abscisic acid-mediated drought stress responses. Plant Physiol **160:** 556–568

**Son O, Cho SK, Kim SJ, Kim WT** (2010) In vitro and in vivo interaction of AtRma2 E3 ubiquitin ligase and auxin binding protein 1. Biochem Biophys Res Commun **393:** 492–497

**Sparkes IA, Runions J, Kearns A, Hawes C** (2006) Rapid, transient expression of fluorescent fusion proteins in tobacco plants and generation of stably transformed plants. Nat Protoc **1:** 2019–2025

**Stone SL** (2014) The role of ubiquitin and the 26S proteasome in plant abiotic stress signaling. Front Plant Sci **5:** 135

**Stone SL, Hauksdóttir H, Troy A, Herschleb J, Kraft E, Callis J** (2005) Functional analysis of the RING-type ubiquitin ligase family of Arabidopsis. Plant Physiol **137:** 13–30

**Suck D, Ficner R** (1996) Structure and function of PCD/DCoH, an enzyme with regulatory properties. FEBS Lett **389:** 35–39

**Tuteja N** (2007) Abscisic acid and abiotic stress signaling. Plant Signal Behav **2:** 135–138

**Verma V, Ravindran P, Kumar PP** (2016) Plant hormone-mediated regulation of stress responses. BMC Plant Biol **16:** 86

**Vierstra RD** (2009) The ubiquitin-26S proteasome system at the nexus of plant biology. Nat Rev Mol Cell Biol **10:** 385–397

**Vierstra RD** (2012) The expanding universe of ubiquitin and ubiquitin-like modifiers. Plant Physiol **160:** 2–14

**Weigel D, Glazebrook J** (2006) Transformation of Agrobacterium using the freeze-thaw method. CSH Protoc **2006:** pdb.prot4666

**Weisberg SJ, Lyakhovetsky R, Werdiger AC, Gitler AD, Soen Y, Kaganovich D** (2012) Compartmentalization of superoxide dismutase 1 (SOD1G93A) aggregates determines their toxicity. Proc Natl Acad Sci USA **109:** 15811–15816

**Yamaguchi-Shinozaki K, Shinozaki K** (2006) Transcriptional regulatory networks in cellular responses and tolerance to dehydration and cold stresses. Annu Rev Plant Biol **57:** 781–803

**Yang L, Liu Q, Liu Z, Yang H, Wang J, Li X, Yang Y** (2016) Arabidopsis C3HC4-RING finger E3 ubiquitin ligase AtAIRP4 positively regulates stress-responsive abscisic acid signaling. J Integr Plant Biol **58:** 67–80

**Yoo SD, Cho YH, Sheen J** (2007) Arabidopsis mesophyll protoplasts: a versatile cell system for transient gene expression analysis. Nat Protoc **2:** 1565–1572

**Yu F, Wu Y, Xie Q** (2015) Precise protein post-translational modifications modulate ABI5 activity. Trends Plant Sci **20:** 569–575

**Yu F, Wu Y, Xie Q** (2016) Ubiquitin-proteasome system in ABA signaling: from perception to action. Mol Plant **9:** 21–33

**Zaarur N, Meriin AB, Bejarano E, Xu X, Gabai VL, Cuervo AM, Sherman MY** (2014) Proteasome failure promotes positioning of lysosomes around the aggresome via local block of microtubule-dependent transport. Mol Cell Biol **34:** 1336–1348

**Zhang H, Cui F, Wu Y, Lou L, Liu L, Tian M, Ning Y, Shu K, Tang S, Xie Q** (2015) The RING finger ubiquitin E3 ligase SDIR1 targets SDIR1-INTERACTING PROTEIN1 for degradation to modulate the salt stress response and ABA signaling in *Arabidopsis*. Plant Cell **27:** 214–227

**Zhang L, Du L, Shen C, Yang Y, Poovaiah BW** (2014) Regulation of plant immunity through ubiquitin-mediated modulation of $Ca^{2+}$-calmodulin-AtSR1/CAMTA3 signaling. Plant J **78:** 269–281

**Zhang Y, Yang C, Li Y, Zheng N, Chen H, Zhao Q, Gao T, Guo H, Xie Q** (2007) SDIR1 is a RING finger E3 ligase that positively regulates stress-responsive abscisic acid signaling in *Arabidopsis*. Plant Cell **19:** 1912–1929

**Zhu JK** (2002) Salt and drought stress signal transduction in plants. Annu Rev Plant Biol **53:** 247–273